AD-A120 048

DRSAR-LEP-L
Tech Lib

TECHNICAL
LIBRARY

AD #120048

MEMORANDUM REPORT ARBRL-MR-03200

(Supersedes IMR No. 725)

COMMENTS ON THE FLIGHT STABILITY OF THE XM736 8-INCH BINARY PROJECTILE

William P. D'Amico, Jr.

October 1982

US ARMY ARMAMENT RESEARCH AND DEVELOPMENT COMMAND
BALLISTIC RESEARCH LABORATORY
ABERDEEN PROVING GROUND, MARYLAND

Approved for public release; distribution unlimited.

Destroy this report when it is no longer needed.
Do not return it to the originator.

Secondary distribution of this report is prohibited.

Additional copies of this report may be obtained from the National Technical Information Service, U. S. Department of Commerce, Springfield, Virginia 22161.

The findings in this report are not to be construed as an official Department of the Army position, unless so designated by other authorized documents.

REPORT DOCUMENTATION PAGE

READ INSTRUCTIONS BEFORE COMPLETING FORM

1. REPORT NUMBER: Memorandum Report ARBRL-MR-05200
2. GOVT ACCESSION NO.
3. RECIPIENT'S CATALOG NUMBER

4. TITLE (and Subtitle): COMMENTS ON THE FLIGHT STABILITY OF THE XM736 8-INCH BINARY PROJECTILE
5. TYPE OF REPORT & PERIOD COVERED: Final
6. PERFORMING ORG. REPORT NUMBER

7. AUTHOR(s): William P. D'Amico, Jr.
8. CONTRACT OR GRANT NUMBER(s)

9. PERFORMING ORGANIZATION NAME AND ADDRESS: U.S. Army Ballistic Research Laboratory, ATTN: DRDAR-BLL, Aberdeen Proving Ground, Maryland 21005
10. PROGRAM ELEMENT, PROJECT, TASK AREA & WORK UNIT NUMBERS: RDT&E 1L162618AH80

11. CONTROLLING OFFICE NAME AND ADDRESS: U.S. Army Armament Research and Development Command, U.S. Army Ballistic Research Laboratory (DRDAR-BL), Aberdeen Proving Ground, MD 21005
12. REPORT DATE: October 1982
13. NUMBER OF PAGES: 70

14. MONITORING AGENCY NAME & ADDRESS (if different from Controlling Office)
15. SECURITY CLASS. (of this report): UNCLASSIFIED
15e. DECLASSIFICATION/DOWNGRADING SCHEDULE

16. DISTRIBUTION STATEMENT (of this Report)

Approved for public release; distribution unlimited.

17. DISTRIBUTION STATEMENT (of the ebetrect entered in Block 20, if different from Report)

18. SUPPLEMENTARY NOTES

This report supersedes BRL IMR No. 725 dated July 1981.

19. KEY WORDS (Continue on reverse side if neceesary and identify by block number)

binary payloads
projectile stability
yawsonde

20. ABSTRACT (Continue on reverse side if necessary and identify by block number)

The recent suspension of testing of the XM736 8-inch binary projectile prompted a review of flight stability for this liquid-filled shell. Yawsonde and aeroballistic range data were reviewed, and the destabilizing effects of the liquid payload and the loose payload canisters were investigated. No dramatic flight instabilities have been observed or are expected, but theoretical models indicate that the reliability of the fuzed projectile may be affected by the liquid payload and/or loose payload canisters. In-flight measurements to determine the projectile

20. ABSTRACT (Cont'd)

motion and fuze performance at high zone charges and high quadrant elevations should be made. Also, aeroballistic range tests should be made to determine the basic flight characteristics of the M509 family of shell.

TABLE OF CONTENTS

LIST OF FIGURES

LIST OF FIGURES (continued)

I. INTRODUCTION

The XM736 is an 8-inch diameter binary projectile. A schematic of the projectile is shown in Figure 1. The forward end of the rear canister and the aft end of the front canister are made of thin steel and form a diaphragm system that is ruptured upon projectile launch (both canisters are partially filled). During in-bore acceleration and free-flight along the trajectory, the inert liquid components in the canisters mix producing an exothermic reaction. During Operational Test II (OT II), several projectile peculiarities were identified and tests were suspended. As a result of this suspension, the design and performance of the XM736 have been re-examined in detail. This report summarizes previous in-flight measurements of the projectile motion and assesses the reliability of the fuzed projectile system in terms of the liquid payload and the loose payload canisters.

II. BACKGROUND

A. Basic Concepts for a Liquid-Filled Projectile

It is well known that a liquid payload can destabilize a projectile. The physical and mathematical explanation of this type of instability was provided by Stewartson[1,2]. Briefly, a natural frequency (an eigenfrequency) of oscillation of the liquid can resonate with the fast precessional frequency of the projectile. In general, the eigenfrequencies depend upon the aspect ratio of the payload container, the container fill ratio, the velocity distribution of the liquid, and the kinematic properties of the liquid. Hence, a complete description of the eigenfrequency history for a particular projectile, liquid payload, and trajectory is a formidable problem.

B. Loose Internal Parts

A relatively new payload-induced instability produced by loose internal components has been analyzed by Murphy[3]. Internal components (such as a steel canister) that have the spin and coning rate of the carrier vehicle may have a motion which is not in phase with the carrier vehicle and thus induce destabilizing effects.

---

1. *K. Stewartson, "On the Stability of a Spinning Top Containing Liquid," Journal of Fluid Mechanics, Vol. 5, Part 4, September 1959, pp. 577-592.*

2. *Engineering Design Handbook, "Liquid-Filled Projectile Design," AMC Pamphlet 706-165, April 1969.*

3. *Charles H. Murphy, "Influence of Moving Internal Parts on Angular Motion of Spinning Projectiles," Journal of Guidance and Control, Vol. 1, No. 2, March-April 1978, pp. 117-122. Also, BRL Memorandum Report No. 2731, February 1977, AD A037338.*

C. Yawsonde Data

The BRL has utilized fuze-configured yawsondes to monitor the motion of spin-stabilized projectiles during flight[4]. Yawsondes are frequently used to determine projectile motion for liquid-filled or loose component projectiles. The projectile motion is presented in terms of Sigma N and Phi Dot versus time. Sigma N is the complement of the angle between a vector drawn to the sun and a vector aligned with the spin axis of the projectile, while Phi Dot is the derivative of the projectile's Eulerian roll angle with respect to the sun plane, i.e., the plane containing the missile's axis and the sun. For cases of large angular motion, oscillations are superimposed upon a normally smooth Phi Dot history.* The mean of such oscillations should be regarded as the actual spin of the projectile. Methods for the partial elimination of these oscillations are available within Reference 5, but the reduction scheme used for the yawsonde data within this report does not incorporate these methods.

D. XM736 Problem Areas

Four problem areas cited as cause for termination of OT II were:

1. Flight instability of the projectile--range personnel observed "large yaw" for Zone 1 and maximum quadrant elevation launches.

2. Low system reliability--trails behind several projectiles were observed shortly after launch.

3. Non-uniform seating of the projectile--several projectiles did not ram.

4. Poor projectile accuracy--low burst heights require fuze set times to be dangerously close to projectile flight times and resulted in several ground impacts without payload ejection.

A complete description or resolution of these potential problem areas is not possible at this time; however, sufficient concern has been raised to critically review loose canister and liquid payload effects. Also, available yawsonde and aeroballistic range data will be reviewed.

---

* *Some Phi Dot data are labeled as spin, but the data formats are all identical.*

4. *W.H. Mermagen and W.H. Clay, "The Design of a Second Generation Yawsonde," Ballistic Research Laboratory Memorandum Report No. 2368, April 1974. AD 780064.*

5. *C.H. Murphy, "Effect of Large High-Frequency Angular Motion of a Shell on the Analysis of Its Yawsonde Records," Ballistic Research Laboratory Memorandum Report No. 2581, February 1976. AD B0094210.*

III. REVIEW OF YAWSONDE DATA

The XM736 has been flight tested with fuze-configured yawsondes at two locations: Dugway Proving Ground (DPG), Utah and Proof and the Experimental Test Establishment (PETE), Nicolet, Quebec, Canada. Yawsonde data for DPG was reported in Reference 6, while data from PETE were reported in References 7, 8, and 9. Some data have not been previously published from these tests and will be provided here. Data from References 5-8 that are pertinent to the potential problem areas will also be included. A review of the yawsonde data will provide a realistic determination for the fast precessional frequency, $\dot{\phi}_1$, and the spin rate, p. These quantities are required to analyze loose canister and liquid payload effects.

A. Data from Dugway Proving Ground (DPG)

A substantial number of XM736 projectiles have been instrumented to monitor simulant payload reaction temperatures and pressures during flight[10,11]. On some occasions, yawsonde instrumented shell were included within the test plan. A group of four shell (BRL 978, 979, 980, and 981) were tested on 27 June 1976. The yawsonde data are shown in Figures 2-11. No abnormal flight behavior was observed. Data for BRL 980 were not received past two seconds (Figures 8 and 9), and data beyond 42s was lost for BRL 981 (Figures 10 and 11). On 27 and 28 September 1976, a group of XM736 shell loaded with reactive simulants

---

6. *W.P. D'Amico, "In-Flight Measurements of Vibrations for the XM736 Binary Projectile," BRL Memorandum Report No. 2793, September 1977. AD B024954L.*

7. *V. Oskay and J.H. Whiteside, "Flight Behavior of 155mm (XM687 Mod I and XM687 Mod II) and 8-Inch (XM736 Mod I) Binary Shell at Nicolet, Canada, During the Winter of 1974-1975," BRL Memorandum Report No. 2608, March 1976. AD B010566L.*

8. *W.H. Mermagen, W.H. Clay, and V. Oskay, "Yawsonde Data from Firings in the Nicolet Winter Test Program 1974-1975," BRL Memorandum Report No. 2612, April 1976. AD B011225L.*

9. *V. Oskay and J.H. Whiteside, "1974-1975 Winter Tests of 155mm (M483 Family) and 8-Inch (M509 Family) High-Capacity Shell at Nicolet, Canada," BRL Memorandum Report No. 2723, January 1977. AD B017015L.*

10. *W.P. D'Amico, W.H. Clay, A. Mark, and W.H. Mermagen, "In-Flight Payload Temperature Measurements for the XM736 Binary Projectile," BRL Memorandum Report No. 2560, November 1975. AD B008702L.*

11. *W.P. D'Amico, "Simulant Reaction Temperature Measurement Via Telemetry for the XM736 at Charge 9," BRL Memorandum Report No. ARBRL-MR-03021, May 1980. AD A086774.*

or solid slugs and wax-filled M106 were tested with a vibration/yawsonde system[11]. All shell were stable, but BRL 1174 (an XM736 with reactive simulants, fired at Change 7 and 800 mils) exhibited a fast precessional mode limit cycle during the final twenty seconds of flight (Figure 12). No unusual spin behavior was seen (Figure 13). Yaw data are shown on an expanded time scale in Figures 14 and 15. During this program two other XM736 shell (also loaded with reactive simulants) were fired at Change 5 and with a quadrant elevation of 750 mils (BRL 1183 and 1184). Both of these shell exhibited a slow precessional mode limit cycle behavior during the terminal portions of their trajectories. The fast precessional mode limit cycle for BRL 1174 was unexpected and is unexplained. Such behavior could be triggered by a loose internal component or the liquid payload.

B. Data from Proof and Experimental Test Establishment (PETE)

A series of high atmospheric density tests were conducted at PETE for the 155mm M483 and 8-inch M509 families of shell. The primary thrust of these tests was to examine the flight stability of these projectiles under the conditions of high launch disturbances and minimum gyroscopic stability. Hence, the yawsonde data were primarily processed for yaw.* The XM736 data from PETE tests were recently processed for both spin and yaw and are presented in Figures 16-35**. Only Round NY18L21 showed any unusual behavior (Figure 21). During the PETE tests, the payload canisters were not keyed to the projectile body. The spin history of Round 18L21 (Figure 21) shows a sudden loss in spin at approximately one second. This is attributed to a non-keyed canister that is abruptly brought up to the spin rate of the projectile body. Evidence such as this led to the use of keyed canisters. Data for Round NY10L1 were lost between 7 and 12 seconds (Figures 24 and 25). Data for Round NY10L6 were not received after 7 seconds.

IV. LIQUID PAYLOAD EFFECTS

The flight performance of a spin-stabilized shell can be adversely affected by a liquid payload. The analysis by Stewartson[1] provides a fundamental description of the instability mechanism.

A. Stewartson Model

Stewartson's theory concerns the flight stability of a spinning shell with a right circular cylindrical cavity either wholly or partially filled with liquid. Results of the theory show that growth

---

* *Preliminary reductions for spin and yaw can be found within Reference 7.*

** *Data plots were provided by B. A. Hodes.*

of the fast precessional component of the projectile's yaw* is possible under adverse combinations of the geometrical and physical characteristics of the projectile and its liquid filler. Instabilities are a consequence of the certain natural frequencies of the liquid being hazardously close to fast precessional frequency of the shell. This can be described as a condition of resonance. When this condition occurs, oscillations of the liquid produce a periodic moment (a couple) on the shell casing and lead to a growth in yaw. Important assumptions are listed below:

1. The projectile spin is constant.

2. The liquid is rotating as a quasi-rigid body at the projectile spin rate.

3. The mass of the liquid is small compared to the total mass of the solid projectile parts.

4. The liquid is incompressible and inviscid.

5. The spin of the liquid and the dimensions of the cylindrical cavity satisfy the condition.

$$a^2p^2 >> \Phi c \quad **$$

where a = cavity radius

p = spin rate of the projectile (and therefore the liquid)

Φ = magnitude of the resolved gravity and drag vectors

$2c$ = height of the cavity

6. The yaw of the liquid/projectile system has the form

$$A = A_o \exp (\tau_I + i\tau_R) pt \qquad (1)$$

where τ_I = growth rate due to the liquid

τ_R = precessional frequency of the liquid/projectile system.

All of these assumptions are relatively well satisfied for a homogeneous liquid payload and the XM736 at long flight times. Corrections for liquid viscosity and spin-up can be incorporated and will be discussed later.

---

* *Normally in ballistic terminology the fast precessional frequency is called the nutational frequency.*

** *The physical significance of this assumption is that centrifugal forces exerted on the liquid due to its spin far outshadow any forces imposed by gravity or drag. A consequence of the assumption is that the liquid (except when the cavity is completely filled) has the shape of a cylinder with a hollow core.*

To describe the behavior of the liquid, recall that it is confined in a container and that its basic motion involves rigid body spin about an axis with fixed direction. Assuming that the axis of the container is subjected to a small disturbance similar to the yawing motion of a shell, it is necessary that the liquid also experiences a disturbance to its basic motion because it must follow the walls of the cavity. Stewartson's solution shows that the liquid conforms to the cavity motion through the exitation of small amplitude oscillations superposed on the rigid body motion. There is an infinite number of discrete frequencies for these oscillations--the natural frequencies (or eigenfrequencies) of the spinning liquid. For an arbitrary motion of the container, all the natural frequencies will be excited, but in varying degrees. If, however, the container performs a yawing motion close to certain of the eigenfrequencies of the liquid, oscillations at this frequency become predominant, that is, a condition of resonance is established. It is this resonance that leads to the instability of a liquid-filled projectile.

It should be emphasized that the oscillations performed by the liquid are of small amplitude and in fact these oscillations can occur in a completely filled container. Sloshing does not occur, but a wave pattern is established in the longitudinal, radial, and circumferential directions of the cavity and there are mode numbers* associated with each direction. For problems of projectile stability, an infinity of the possible longitudinal (j) and radial (n) modes are theoretically significant, but only the first circumferential (m) mode is important. This circumstance occurs since only the m=1 pressure fluctuations produce a net couple on the projectile.

Reference 2 provides a numerical tabulation of the eigenfrequencies (τ_{nj}), but in a functional form* *

$$\tau_{nj} = \tau_{nj}\,[(c/a)/(2j+1),\ b^2/a^2] \ . \qquad (2)$$

where n = radial mode number (the number of modes in the radial wave pattern), n = 1, 2, ...

j = longitudinal wave number (2j+1 = number of modes in the longitudinal wave pattern), j = 0, 1, 2 .....

τ_{nj} = the non-dimensional eigenfrequency of the nj^{th} mode

2a = diameter of the cavity

---

* *These can be thought of as fundamental wave patterns and harmonics.*

** *It is always assumed that m=1, so the notation is shortened to only n and j.*

$2b$ = diameter of the cylindrical air core

$2c$ = cavity length

Several aspects of Equation (2) should be noted. First, the eigenfrequencies of the liquid are dependent upon the cavity geometry through the ratios c/a and b^2/a^2. The ratio b^2/a^2 is the air volume in the cavity expressed as a fraction of the total cavity volume. Hence $(1 - b^2/a^2)$ is the fraction of the cavity occupied by liquid, i.e., the fill ratio. Next, note that the eigenfrequencies depend upon the longitudinal mode number through the ratio $c/a(2j+1)$ appearing as a variable in τ_{nj}. This is a fortunate circumstance, because once τ_{nj} is known for a set of fixed values of $c/a(2j+1)$, b^2/a^2, and n, the eigenfrequencies are known for all longitudinal modes for which $c/a(2j+1)$ equals the set value. Finally, Equation (2) shows the frequencies τ_{nj} are independent of the spin, so long as it is constant.

The standard expressions for the fast and slow precessional frequencies[2] of an empty projectile are:

$$\tau_{NU} = \dot{\phi}_1/p = (I_x/2I_y)(1 + \sigma) \tag{3}$$

and

$$\tau_{PR} = \dot{\phi}_2/p = (I_x/2I_y)(1 - \sigma) \tag{4}$$

where $$\sigma = (1 - 1/s_g)^{\frac{1}{2}} \tag{5}$$

s_g = gyroscopic stability factor

The dimensional frequencies $\dot{\phi}_1$, $\dot{\phi}_2$, and p can be obtained from yawsonde data or they may be estimated by using aeroballistic range data. A simple statement of the Stewartson instability criterion is:

$$(\tau_{NU} - \tau_{nj})^2 < \rho a^6 (2R_{nj})^2 / cI_x \sigma \tag{6}$$

The liquid density is ρ, while the factor R_{nj} provides the magnitude of the destabilizing liquid moment.* Each τ_{nj} has a particular value for R_{nj}. From the inequality (6), if τ_{nj} and τ_{NU} are vastly different, then the projectile will be stable. The inequality (6) dictates if τ_{nj} and τ_{NU} are sufficiently close to produce a resonant condition. Under such circumstances, the Stewartson theory can then predict the yaw growth rate due to the liquid.

The effects of liquid viscosity were incorporated into the Stewartson model by Wedemeyer[12]. Wedemeyer used classical boundary layer techniques to determine displacement surfaces along the cylinder end and side walls. The inviscid geometry was modified according to these displacement thicknesses and a viscous corrected eigenfrequency, τ^{V}_{nj}, was derived. The stability analysis for the projectile/liquid system was repeated with τ_{nj} replaced by τ^{V}_{nj} (this eigenvalue has real and imaginary parts). The viscous corrected model will be called the Stewartson-Wedemeyer (S-W) theory.

The simple correction provided by τ^{V}_{nj} is quite ingenious, but the ramifications are subtle and not clearly understood. In short, this correction seems to work for a range of Reynolds numbers: $10^3 < Re < 10^6$. The S-W theory has been tested using laboratory gyroscopes and has in general formed the basis of projectile design practices. However, the S-W theory has not been tested against either large or small caliber projectile data. Many of the restrictions and assumptions are unsatisfactory, and the application of the S-W theory must be done with some reservation. The impact of epicyclic motion at finite but small amplitudes of yaw may produce liquid/projectile behavior not predicted or anticipated by the S-W theory which is linear. Murphy has recently developed a method to compute the flight stability of a liquid-filled shell[13]. This method utilizes Wedemeyer's viscous correction, but provides a better model for the projectile dynamics than the S-W theory. The methods of Reference 13 will be used later in this report.

The assumption of rigid body rotation of the liquid within a projectile at early flight times is unrealistic. The yawsonde records clearly show a rapid decrease in projectile spin after shot exit. The decrease in projectile spin is produced by spin-up of the liquid. Wedemeyer has analyzed spin-up from rest in a cylinder[14] and this model can be applied to a projectile. Substantial work by several investigators has been accomplished on the effects

---

* *R_{nj} is tabularized in Reference 2.*

12. *E. H. Wedemeyer, "Viscous Corrections to Stewartson's Stability Criterion," BRL Report No. 1325, June 1966. AD 489687.*

13. *C. H. Murphy, "Angular Motion of a Spinning Projectile with a Viscous Liquid Payload," BRL Technical Report in publication.*

14. *E. H. Wedemeyer, "The Unsteady Flow Within a Spinning Cylinder," BRL Report No. 1225, October 1965. AD 431846.*

of liquid spin-up within a projectile[15-20]. A major result from these efforts is the calculation of the liquid eigenfrequencies (CR+iCI) during spin-up for a viscous fluid. At present, however, it is not possible to compute the associated liquid moment. The real part of the time-dependent eigenfrequency is CR and the asymptotic value for CR at long times is equal to the real part of τ^{V}_{nj}. A method for the calculation of CR (as well as the imaginary part CI) has been accomplished using the techniques developed within Reference 18. The Stewartson mechanism for instability still applies during spin-up, i.e., resonance will occur for $\tau_{NU} \cong$ CR. (The S-W instability criteria cannot be applied.) Only hueristic arguments can be used to judge the potential danger of a spin-up instability. For example, if dCR/dt is large, then the resonant condition of CR = τ_{NU} will be short lived and projectile stability may not be affected. Also, higher values for n and j typically will produce smaller destabilizing moments. Both of these concepts should be carefully exercised and should be confirmed by actual projectile tests, however. For the XM736, CR histories can be used to define the time frame of applicability of the S-W model. In general, the analyses for CR are linear (limited to small angles) and form at best a crude approximation to the actual binary payload of the

---

15. *C. W. Kitchens, Jr., and N. Gerber, "Prediction of Spin-Decay of Liquid-Filled Projectiles," BRL Report No. 1996, July 1977. AD A043275.*

16. *C. W. Kitchens, Jr., and R. Sedney, "Conjecture for Anomalous Spin Decay of the 155mm Binary Shell (XM687)," BRL Report No. 2026, October 1977. AD A050311.*

17. *A. Mark, "Measurements of Angular Momentum Transfer in Liquid-Filled Projectiles," BRL Technical Report No. ARBRL-TR-02029, November 1977. AD A051056.*

18. *C. W. Kitchens, Jr., N. Gerber, and R. Sedney, "Oscillations of a Liquid in a Rotating Cylinder: Part I. Solid-Body Rotation," BRL Technical Report No. ARBRL-TR-02081, June 1978. AD A057759.*

19. *Y. M. Lynn, "Free Oscillations of a Liquid During Spin-Up," BRL Report No. 1663, August 1973. AD 769710.*

20. *W. P. D'Amico, W. H. Clay, and A. Mark, "Yawsonde Data for M687-Type Projectiles with Application to Rapid Spin Decay and Stewartson-Type Spin-Up Instabilities," BRL Memorandum Report No. ARBRL-MR-03027, June 1980. AD A089646.*

XM736 which contains burst discs and reacting fluids. Also, the determination of CR is limited to completely filled canisters.

B. Predictions from Available Models

"Steady State" Model

The range of τ_{NU} for the XM736 can be estimated from Equation (2) if a range of s_g is assumed. For the XM736, a nominal value for I_x/I_y is 0.12 (see Reference 6, pp. 16). If $1 < s_g < 5$, then $0 < \sigma < 0.89$ and

$$0.06 < \tau_{NU} < 0.113.$$

An examination of available yawsonde data yields:

$$0.097 < \tau_{NU} < 0.136 .$$

The largest observed value for τ_{NU} occurred for BRL 1174 (Figures 12 - 15).

The XM736 payload canisters are initially partially-filled but the exothermic reaction yields fill ratios close to 100 percent. Table 1 was derived from the Stewartson tables and lists values for $(c/a)/(2j+1)$ that have been scaled by the $(c/a)/(2j+1)$ value corresponding to a fill ratio 100 percent ($b^2/a^2 = 0$). A range of τ_{nj} was selected that is pertinent to the XM736. Table 1 indicates that τ_{nj} is only a weak function of fill ratio for n=1 and n=2 when $0 \leq \tau_{nj} \leq 0.15$ and $b^2/a^2 \leq .05$. Under these circumstances, the XM736 canisters will be assumed to be completely filled. Moreover, the assumption of a completely filled cylinder would be required for the calculation of spin-up eigenfrequency (CR) histories.

The interior dimensions of the canisters after rupture of the burst discs are:

$$\text{half height} = c = 30.363 \text{ cm}$$

$$\text{radius} = a = 7.569 \text{ cm}$$

The Stewartson table of eigenfrequencies is provided within Table 2 for a completely filled cylinder ($b^2/a^2 = 0$). The aspect ratios where resonance can occur are:

j	0	1	2	3	4	5	6
$\frac{c/a}{2j+1}$	4.011	1.337	0.802	0.573	0.446	0.365	0.309

Resonant behavior is not possible for $j>6$ if $n \leq 3$. Resonant aspect ratios for $n>3$ will not be considered. The following modal combinations (n,j) are possible for the XM736 if $0 \leq \tau_{nj} < 0.50$

$n = 1,\ j = 1,\ \tau_{nj} \approx 0.25$ $\qquad$ $n = 3,\ j = 4,\ \tau_{nj} \approx 0.26$

$n = 2,\ j = 2,\ \tau_{nj} \approx 0.37$ $\qquad$ $n = 3,\ j = 5,\ \tau_{nj} \approx 0.12$

$n = 2,\ j = 3,\ \tau_{nj} \approx 0.14$ $\qquad$ $n = 3,\ j = 6,\ \tau_{nj} \approx 0.00$

$n = 3,\ j = 3,\ \tau_{nj} \approx 0.41$

For $\tau_{NU} = 0.12$ some of these modes could be dangerous, but the τ_{nj} values for the (1,1), (2,2), (3,3), (3,4), and (3,6) modes are relatively far removed from $\tau_{NU} = 0.12$.

Calculations for the yaw growth rate were made for a range of coning frequencies between 0.11 and 0.15 using the methods developed by Murphy. A spin rate of 117.5 Hz (an average spin for the 40-50 second time frame) was used. Also, it was assumed that the payload compartment was completely filled with water. Figure 36 shows the results. Since BRL 1174 had τ=0.12, the growth rate due to the liquid would be approximately 0.07 1/sec if aerodynamic effects are neglected. During the 40-50 second time frame K_1 doubled resulting in a yawsonde determined growth rate of [ln (2)] / 10 = 0.069 1/sec. The agreement between the computed and measured growth rates is quite surprising and further comments will be delayed until aerodynamic effects are determined within a later section.

C. Spin-Up Calculations

The application of the S-W theory is only valid when the liquid is spinning as a quasi-rigid body with the projectile. Using the techniques outlined in References 14 and 18, the time required by the liquid to achieve rigid body rotation and the eigenfrequency history during spin-up can be computed. Such estimates can be used to determine applicability of steady state theories. Note that the period of rapid despin of the projectile as seen from yawsonde data cannot be used to identify when spin-up of the liquid is complete or when the spin-up eigenfrequency is approximately equal to the S-W eigenfrequency. A spin-up eigenfrequency history (CR versus time) must be computed. At long flight times CR will tend towards the steady state eigenfrequency. CR can be computed for a variable spin rate. Under such conditions, the spin-up eigenfrequency is scaled by the local spin rate and is called CR*.

Spin-up eigenfrequency histories were computed for the (2,3) and (3,5) modes using the spin rate from BRL 1174. The CR* estimates for the (2,3) mode crossed the steady state eigenfrequency (τ_{23}=0.138) after 25 seconds of flight (Figure 37). The CR* estimate for the (3,5) mode crossed the steady state eigenfrequency (τ_{35}=0.120) after 30 seconds of flight (Figure 38).

From the spin-up calculations, however, it is apparent that the steady state theory is applicable only over the final portions of the trajectory of BRL 1174. It is quite possible that either the (2,3) or the (3,5) modes could induce a fast precessional mode instability. All of the predictions of eigenfrequency behavior are obtained from linearized theories, and it is highly probable that nonlinear effects would shift the locations of the predicted τ_{nj} and CR* histories. Also, nonlinear effects would modify the yaw growth. At present nonlinear corrections are not available in an analytical or empirical form for any of the models.

V. LOOSE CANISTER EFFECTS

Loose internal components can adversely affect the stability of a spin-stabilized projectile.[3] The payload canisters within the XM736 are very large and tolerances between the canisters and the projectile body are necessary to permit assembly and payload ejections. Within Reference 3, two internal motions of a loose payload component are modeled. One model assumes that the component is coning within the projectile. The coning motion is quite small, but this motion is not in phase with the projectile motion. A second model assumes that the internal component performs a rolling motion within the projectile (a hula-hoop type motion).

Past experience has shown that roll pins may prevent payload slippage but such pins do not prevent coning or center of gravity motions. The key located between the forward canister and the XM736 projectile body should prevent center of gravity motions, but a coning motion could occur if the key or keyway were sufficiently deformed. The equation governing the growth of the fast precessional mode as derived in Reference 3 is:

$$\dot{K}_1 = \lambda_F K_1 + (\dot{\phi}_1 B_\gamma \gamma \sin\phi_\gamma)/(2I_y\dot{\phi}_1 - I_x p), \tag{7}$$

where: K_1 = amplitude of the fast precessional mode

λ_F = aerodynamic damping of the rigid projectile for the fast precessional mode

$\dot{\phi}_1$ = fast precessional frequency

$B_\gamma = I_{xc}p_c - I_{yc}\dot{\phi}_1$

γ = cant angle of the loose component

ϕ_γ = phase angle between the cant plane and the angle of attack plane (usually ϕ_γ is assumed to be 45 degrees)

I_x, I_y = axial and transverse moments of inertia of the complete projectile (without liquid)

I_{xc}, I_{yc} = axial and transverse moments of inertia of the loose component

p = projectile spin rate (also the component spin rate)

The forward payload canister will be considered as loose and manufacturing tolerances will be used to compute γ. The effect of the smaller rear canister will be neglected, and the canisters will be considered as empty.

Mass of forward canister:	26.1 kg
Distance between the projectile and forward canister center of gravities:	8.8 cm
Radial tolerance between canister and projectile body:	0.050 cm (0.020 inch)
Moments of Inertia:	
I_x, I_y:	0.502, 4.21 kg·m^2
I_{xc}, I_{yc}:	0.169, 0.892 kg·m^2
Fast precessional Frequency, $\dot{\phi}_1$:	14 hz
Spin Rate, p:	115 hz
Cant Angle, γ:	2×10^{-3} rad

For $\lambda_1 = 0$ within Equation (7), $\dot{K}_1 = 0.0143$ rad/sec. Rescaling this growth rate for $K_1 = 2$ deg (see Figure 14, 45 - 50 second time frame), then $\dot{K}_1/K_1 = 0.41$ sec^{-1}.

VI. ESTIMATES FOR FAST PRECESSIONAL MODE AERODYNAMIC DAMPING

Aerodynamic range data are not available for the M509-type shell. Only a few prototype XM509 shell were fired through the BRL Transonic Range facility for the determination of aerodynamic parameters. Due to substantial differences in exterior shape of the tested rounds and the present M509 and XM736 hardware, these data are not reliable. An estimate of the fast precessional mode damping is required for comparison with undamping rates predicted by liquid or loose canister effects.

A modified point mass trajectory (standard atmospheric conditions only) was computed for an M509 with the launch conditions of BRL 1174. At a time of flight of 40 seconds, trajectory estimates were: spin rate = 126.5 rev/sec, velocity = 257.8 m/sec, and Mach number = 0.77. Using these

quantities as inputs, aeroballistic range data for 155mm models of the 8-inch XM650E2 will be used to estimate a typical level of damping.[21] From Table 2 of Reference 21, the slow and fast mode damping for M = 0.762, $\lambda_S + \lambda_F$ = -0.411×10^{-3} per caliber. Conversion of $\lambda_F + \lambda_S$ into the dimensions used to predict liquid and loose payload effects is:

$$\lambda_S + \lambda_F = \frac{(\lambda_I \ 1/\text{cal}) \quad (\text{Velocity m/s})}{(\text{model diameter m/cal})}$$

The gyroscopic stability factor, s_g, for the aeroballistic range model at M = 0.762 was 1.32. If the presence of the liquid is neglected, estimates for s_g, $\dot{\phi}$, and the aerodynamic damping and Magnus moments, $\hat{H}$ and $\hat{T}$, can be made.[22]

$$s_g = (\dot{\phi}_1 + \dot{\phi}_2)^2/4(\dot{\phi}_1\dot{\phi}_2 - \lambda_F\lambda_S) = 9.8 \tag{8}$$

$$\dot{\phi} = (I_x/I_y)\ (\dot{\phi}_1 + \dot{\phi}_2) = 120 \text{ Hz} \tag{9}$$

$$\hat{H} = -\ (\lambda_F + \lambda_S) = 0.683 \text{ 1/sec} \tag{10}$$

$$\hat{T} = -\ (\dot{\phi}_2\lambda_F/\dot{\phi}_1 + \lambda_S)/(1 + \dot{\phi}_1/\dot{\phi}_2) = 0.601 \text{ 1/sec} \tag{11}$$

VII. IMPACT OF PAYLOAD-INDUCED INSTABILITIES UPON FUZE OPERATION

The accurate operation of a time fuze is critical for the XM736 for proper payload ejection to occur. The M577 fuze is employed with the XM736 and concerns were raised during DT II and OT II tests as to the reliability of the XM736/M577 system. A failure of the M577 with the XM509 was documented within Reference 23. This particular failure was produced by a malfunction

---

21. *Maynard J. Piddington, "The Aerodynamic Characteristics of the 155mm Model of the 8" XM650E2," BRL MR 2538, October 1975, AD B007751L.*

22. *C. H. Murphy, "Free Flight Motions of Symmetric Missiles," BRL R 1216, APG, July 1963, AD A42757.*

23. *Dr. Gerard G. Lowen, Dr. Frederick R. Tepper, "Report on Preliminary Failure Investigation of XM509/M577 System and Recommendations for In-Depth Study," Ammunition Engineering Directorate Technical Report 4545, Picatinny Arsenal, Dover, NJ, August 1973.*

of the safe separation device (SSD). Tests also showed that the operation of the fuze was sensitive to the eccentricity between the projectile spin axis and the longitudinal geometric axis. For example, at Zone 5W, eccentricities greater than 0.008 inch produced 27% duds. If the forward canister (without liquid) is shifted outward to the maximum radial tolerance, an off-set of 0.008 inch is produced! Also, the performance of the SSD can be impaired by unexpectedly large or fast yawing motion. The yaw experienced by BRL 1174 was not large in amplitude, but the fast precessional motion was substantially faster than the expected slow precessional motion (14 hz compared to 1.5 hz). The force exerted on the fuze and its various components by the yawing motion is proportional to the square of the yawing frequency, hence the motion experienced by BRL 1174 produced forces 100 times larger than expected. Recently, an instrumentation technique has been developed and successfully tested for the in-flight measurement of timer accuracy, SSD function, and firing pin release of an M509/M577 system.[24] This technique could be utilized to examine fuze operation under actual flight conditions for the XM736/M577 system.

VIII. DISCUSSION

Yawsonde and aeroballistic range data have been reviewed for the XM736 and are inadequate to provide complete and/or accurate inputs to theories which estimate destabilizing effects for liquid payloads and loose internal parts. It was found that a steady state, Stewartson-type instability could have been observed during the last twenty seconds of flight for one projectile. Using the estimates for damping and Magnus moments, the liquid-induced growth rate was recomputed for this case. Also, a sensitivity study was made for a $\pm$0.25% change in the aspect ratio of the cylindrical payload compartment. The results are shown in Figure 39. For a coning frequency of 0.12, the inclusion of the aerodynamic terms has eliminated the destabilizing effects of the liquid. As stated earlier, the aerodynamics are not well determined, and it is not known whether the estimates of Figure 39 better represent the flight case than the earlier estimates of Figure 36 where aerodynamics effects were neglected.

A summary of calculated or observed yaw growth rates are provided below:

Liquid-induced (without aerodynamic effects): 0.07 1/sec

Liquid-induced (with aerodynamic effects): none

Loose canister (without aerodynamic effects): 0.41 1/sec

Yawsonde data for BRL 1174: 0.07 1/sec

It would have been fortuitous that a careful re-examination of the above sources could provide an adequate explanation for the flight behavior of BRL 1174. Such is not the case. The slight growth in yaw which was observed during the 40-50 second time frame could be produced by aeroballistic forces and moments. However, flight experiences with solid payload shell have never

---

24. *W. H. Clay and J. B. Harmon, "Telemetry Test Results with the M509/M577 Projectile/Fuze System," BRL Memorandum Report in publication.*

produced a fast mode limit cycle. Even projectiles that are poorly damped for the fast mode, such as the M549, do not exhibit the motion of BRL 1174. In some cases, the fast mode amplitude generated at launch will persist until impact, but for BRL 1174 the fast mode amplitude was zero prior to 40 seconds into the flight. This type of fast mode instability, however small in amplitude, suggests a payload projectile interaction.

It is important that projectile designers appreciate the potential dangers of loose internal parts and liquid payloads. For a projectile such as the XM736, the loose canister estimate is an upper bounds based upon a totally ineffective canister key. A marginal design for the key could result in lower growth rates, but the potential for yaw instabilities does exist. The liquid payload design can be much more subtle, since many possible modes of instability exist. For the flight of BRL 1174, a minor Stewartson-like instability may have occurred, but the impact on the performance/reliability of the projectile system is serious. Aerodynamic damping was estimated as barely sufficient to prevent a growth in yaw. A slight change in flight conditions or external body geometry could upset such a delicate balance. It is coincidental that substantial fuze/expelling system failures were experienced by the XM736 for high quadrant elevation/high zone charge conditions. Behavior similar to that of BRL 1174 could impair the operation of mechanical time fuzes such as the M577, especially if the flight conditions reduce aeroballistic damping effects and allow a liquid-induced growth in yaw.

IX. CONCLUSIONS

1. A review of all yawsonde data for the XM736 showed a single case where a small amplitude, fast precessional mode, limit cycle occurred.

2. Calculations of liquid-induced yaw growth roughly agree with the yawsonde observed yaw growth leading to the limit cycle behavior.

3. Calculations of loose canister effects indicate large yaw growth rates for improperly keyed canisters.

4. Aerodynamic range tests and yawsonde tests should be conducted to improve the data base for the M509 family of shell to provide basic inputs to shell designers.

X. ACKNOWLEDGEMENTS

The author is indebted to Ms. B. A. Hodes for retrieving and plotting yawsonde data from archived records; to Ms. J. Bartos for coding and running the time-dependent spin option in the calculation of unsteady eigenfrequencies; and to Mr. J. Bradley for encoding aerodynamic effects into the estimation of liquid-induced growth rates.

TABLE 1. Scaled Aspect Ratio versus Fill Ratio

$1 - b^2/a^2$: Fill Ratio (%)

τ_{1j}	100	98	95	90
		First Radial Mode (n=1)		
.00	1	.999	.999	.986
.05	1	.999	.996	.986
.10	1	1.000	.997	.987
.15	1	1.001	.999	.989
		Second Radial Mode (n=2)		
τ_{2j}				
.00	1	.994	.973	.923
.05	1	.996	.974	.924
.10	1	.996	.974	.925
.15	1	.997	.976	.927
		Third Radial Mode (n=3)		
τ_{3j}				
.00	1	.984	.939	.861
.05	1	.985	.940	.861
.10	1	.983	.938	.862
.15	1	.986	.942	.863

TABLE 2. Fluid Frequencies and Residues for Various Cylindrical Cavities of Height 2c and Diameter 2a, and various Fill-Ratios b^2/a^2 where 2b is the Diameter of the Air Column

$b^2/a^2 = 0.00$

	n=1		n=2		n=3	
τ_{nj}	$\frac{c}{a(2j+1)}$	2R	$\frac{c}{a(2j+1)}$	2R	$\frac{c}{a(2j+1)}$	2R
.00	.995	.000	.478	.0000	.310	.0000
.02	1.018	.058	.490	.0070	.319	.0019
.04	1.042	.118	.503	.0144	.327	.0040
.06	1.066	.181	.516	.0223	.336	.0062
.08	1.091	.246	.530	.0307	.345	.0086
.10	1.117	.313	.544	.0396	.355	.0111
.12	1.144	.382	.559	.0491	.364	.0139
.14	1.172	.454	.574	.0591	.375	.0168
.16	1.201	.528	.590	.0697	.385	.0198
.18	1.231	.604	.607	.0809	.397	.0231
.20	1.262	.682	.624	.0928	.408	.0266
.22	1.294	.762	.642	.1054	.420	.0304
.24	1.328	.845	.661	.1187	.433	.0344
.26	1.363	.930	.680	.1328	.446	.0387
.28	1.399	1.017	.700	.1478	.460	.0433
.30	1.437	1.107	.722	.1636	.475	.0481
.32	1.478	1.200	.745	.1804	.490	.0533
.34	1.521	1.295	.769	.1981	.506	.0589
.36	1.565	1.392	.794	.2169	.523	.0649
.38	1.612	1.491	.820	.2369	.541	.0714
.40	1.662	1.593	.848	.2581	.561	.0783
.42	1.715	1.698	.878	.2805	.582	.0858
.44	1.771	1.805	.910	.3043	.603	.0938
.46	1.831	1.914	.944	.3296	.626	.1024
.48	1.895	2.026	.980	.3566	.651	.1118
.50	1.963	2.142	1.019	.3853	.678	.1220

REFERENCES

1. K. Stewartson, "On the Stability of a Spinning Top Containing Liquid," Journal of Fluid Mechanics, Vol. 5, Part 4, September 1959, pp. 577-592.

2. Engineering Design Handbook, "Liquid-Filled Projectile Design," AMC Pamphlet 706-165, April 1969.

3. Charles H. Murphy, "Influence of Moving Internal Parts on Angular Motion of Spinning Projectiles," Journal of Guidance and Control, Vol. 1, No. 2, March-April 1978, pp. 117-122. Also, BRL Memorandum Report No. 2731, February 1977. AD A037338.

4. W.H. Mermagen and W.H. Clay, "The Design of a Second Generation Yawsonde," Ballistic Research Laboratory Memorandum Report No. 2368, April 1974. AD 780064.

5. C.H. Murphy, "Effect of Large High-Frequency Angular Motion of a Shell on the Analysis of Its Yawsonde Records," Ballistic Research Laboratory Memorandum Report No. 2581, February 1976. AD B0094210.

6. W.P. D'Amico, "In-Flight Measurements of Vibrations for the XM736 Binary Projectile," BRL Memorandum Report No. 2793, September 1977. AD B024954L.

7. V. Oskay and J.H. Whiteside, "Flight Behavior of 155mm (XM687 Mod I and XM687 Mod II) and 8-Inch (XM736 Mod I) Binary Shell at Nicolet, Canada, During the Winter of 1974-1975," BRL Memorandum Report No. 2608, March 1976. AD B010566L.

8. W.H. Mermagen, W.H. Clay, and V. Oskay, "Yawsonde Data from Firings in the Nicolet Winter Test Program 1974-1975," BRL Memorandum Report No. 2612, April 1976. AD B011225L.

9. V. Oskay and J.H. Whiteside, "1974-1975 Winter Tests of 155mm (M483 Family) and 8-Inch (M509 Family) High-Capacity Shell at Nicolet, Canada," BRL Memorandum Report No. 2723, January 1977. AD B017015L.

10. W.P. D'Amico, W.H. Clay, A. Mark, and W.H. Mermagen, "In-Flight Payload Temperature Measurements for the XM736 Binary Projectile," BRL Memorandum Report No. 2560, November 1975. AD B008702L.

11. W.P. D'Amico, "Simulant Reaction Temperature Measurement Via Telemetry for the XM736 at Charge 9," BRL Memorandum Report No. ARBRL-MR-03021, May 1980. AD A086774.

12. E.H. Wedemeyer, "Viscous Corrections to Stewartson's Stability Criterion," BRL Report No. 1325, June 1966. AD 489687.

13. C.H. Murphy, "Angular Motion of a Spinning Projectile with a Viscous Liquid Payload," BRL Technical Report in publication.

14. E.H. Wedemeyer, "The Unsteady Flow Within a Spinning Cylinder," BRL Report No. 1225, October 1965. AD 431846.

15. C.W. Kitchens, Jr., and N. Gerber, "Prediction of Spin-Decay of Liquid-Filled Projectiles," BRL Report No. 1996, July 1977. AD A043275.

16. C.W. Kitchens, Jr., and R. Sedney, "Conjecture for Anomalous Spin Decay of the 155mm Binary Shell (XM687)," BRL Report No. 2026, October 1977. AD A050311

17. A. Mark, "Measurements of Angular Momentum Transfer in Liquid-Filled Projectiles," BRL Technical Report No. ARBRL-TR-02029, November 1977. AD A051056.

18. C.W. Kitchens, Jr., N. Gerber, and R. Sedney, "Oscillations of a Liquid in a Rotating Cylinder: Part I. Solid-Body Rotation," BRL Technical Report No. ARBRL-TR-02081, June 1978. AD A057759.

19. Y.M. Lynn, "Free Oscillations of a Liquid During Spin-Up," BRL Report No. 1663, August 1973. AD 769710.

20. W.P. D'Amico, W.H. Clay, and A. Mark, "Yawsonde Data for M687-Type Projectiles with Application to Rapid Spin Decay and Stewartson-Type Spin-Up Instabilities," BRL Memorandum Report No. ARBRL-MR-03027, June 1980. AD A089646.

21. Maynard J. Piddington, "The Aerodynamic Characteristics of the 155mm Model of the 8" XM650E2," BRL Memorandum Report No. 2538, October 1975. AD B007751L.

22. C.H. Murphy, "Free Flight Motions of Symmetric Missiles," BRL Report No. 1216, Aberdeen Proving Ground, MD, June 1963. AD A42757.

23. Dr. Gerard G. Lowen, Dr. Frederick R. Tepper, "Report on Preliminary Failure Investigation of XM509/M577 System and Recommendations for In-Depth Study," Ammunition Engineering Directorate Technical Report 4545, Picatinny Arsenal, Dover, NJ, August 1973.

24. W.H. Clay and J.B. Harmon, "Telemetry Test Results with the M509/M577 Projectile/Fuze System," BRL Memorandum Report in publication.

LIST OF SYMBOLS

a	radius of a cylindrical cavity
A	amplitude of projectile yaw, Equation (1)
b	radius of a cylindrical air core
B_γ	$I_{xc}p_c - I_{tc}\phi_1$
c	half height of a cylindrical cavity
CR, CI	Real, imaginary parts of the spin-up eigenfrequency
CR*, CI*	Real, imaginary parts of the spin-up eigenfrequency when scaled to the instantaneous spin rate
i	$(-1)^{1/2}$
I_x, I_y	axial, transverse moment of inertia of the projectile
I_{xc}, I_{yc}	axial, transverse moment of inertia of the loose component
j	mode number of the axial wave pattern
K_j	magnitude of the jth modal arm, j=1,2
$(\dot{K}_1)_{n,j}$	growth rate of the fast precessional mode produced by the nj^{th} liquid mode
M	Mach number
n	mode number of the radial wave pattern
p	spin frequency
R_{nj}	A quantity that describes the magnitude of the liquid moment
Re	Reynolds number
s_g	Gyroscopic stability factor
λ_F, λ_S	aerodynamic damping of the fast or slow precessional mode
ν	kinematic viscosity of the liquid
ρ	liquid density
σ	defined within Equation (5)
ϕ_j	$\phi_{j0} + \dot{\phi}_j t$, the orientation angle of the jth modal arm, j=1,2

LIST OF SYMBOLS (continued)

ϕ_{j0}	initial orientation angle of the jth modal arm, j=1,2
$\dot{\phi}_j$	frequency of the jth modal arm, j=1,2 (it is assumed that $\dot{\phi}_1 > \dot{\phi}_2$, i.e., the 1-arm is the fast arm)
ϕ_γ	cant angle of the loose component
Φ	magnitude of the resolved gravity and drag vectors
τ_I	nondimensional growth rate of the projectile
τ_{nj}	nondimensional inviscid liquid eigenfrequency of the nj^{th} mode
τ_{NU}	nondimensional nutational frequency of the empty gyroscope
τ_{nj}^{v}	viscous corrected eigenfrequency

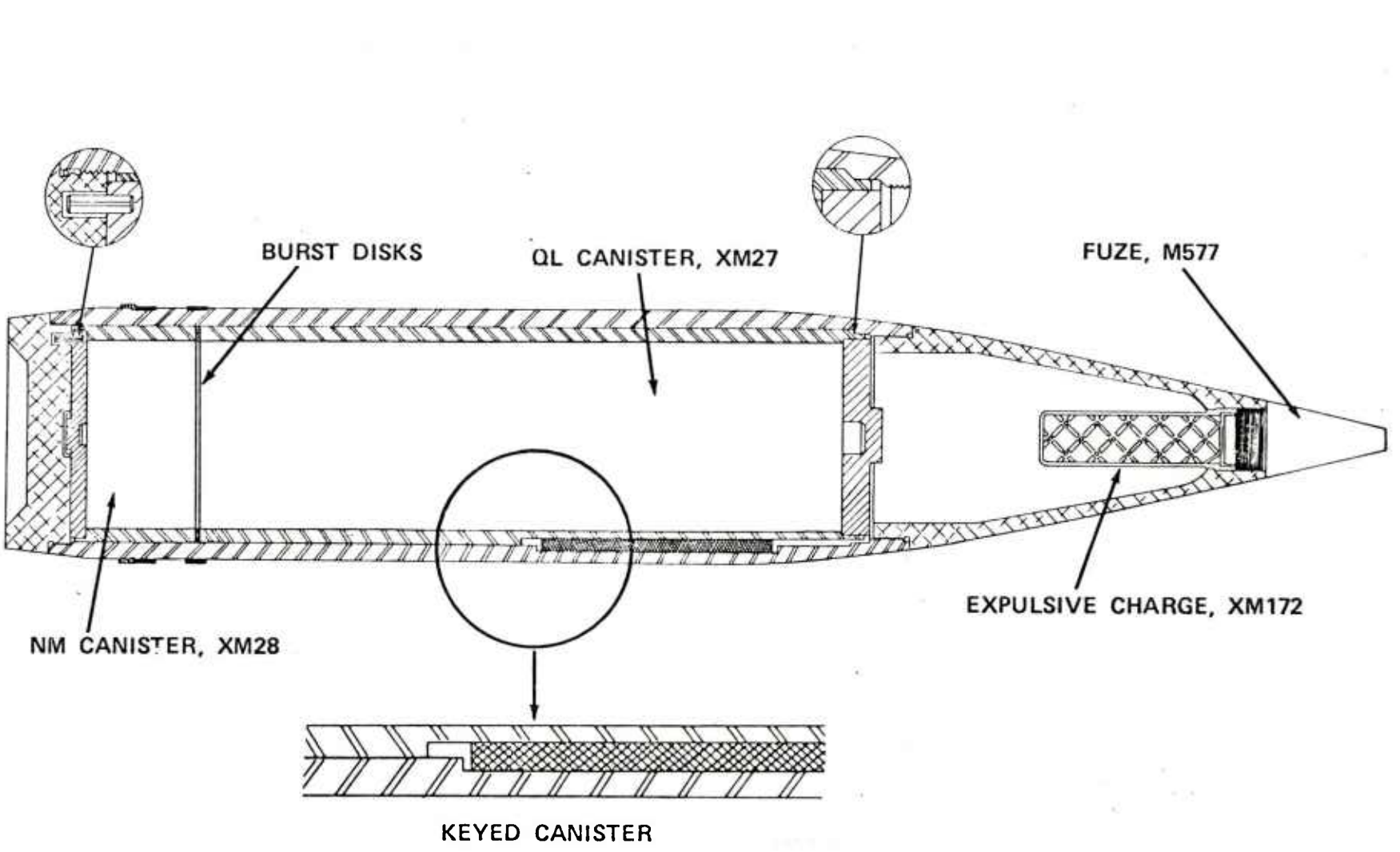

Figure 1. Schematic of the XM736 binary projectile.

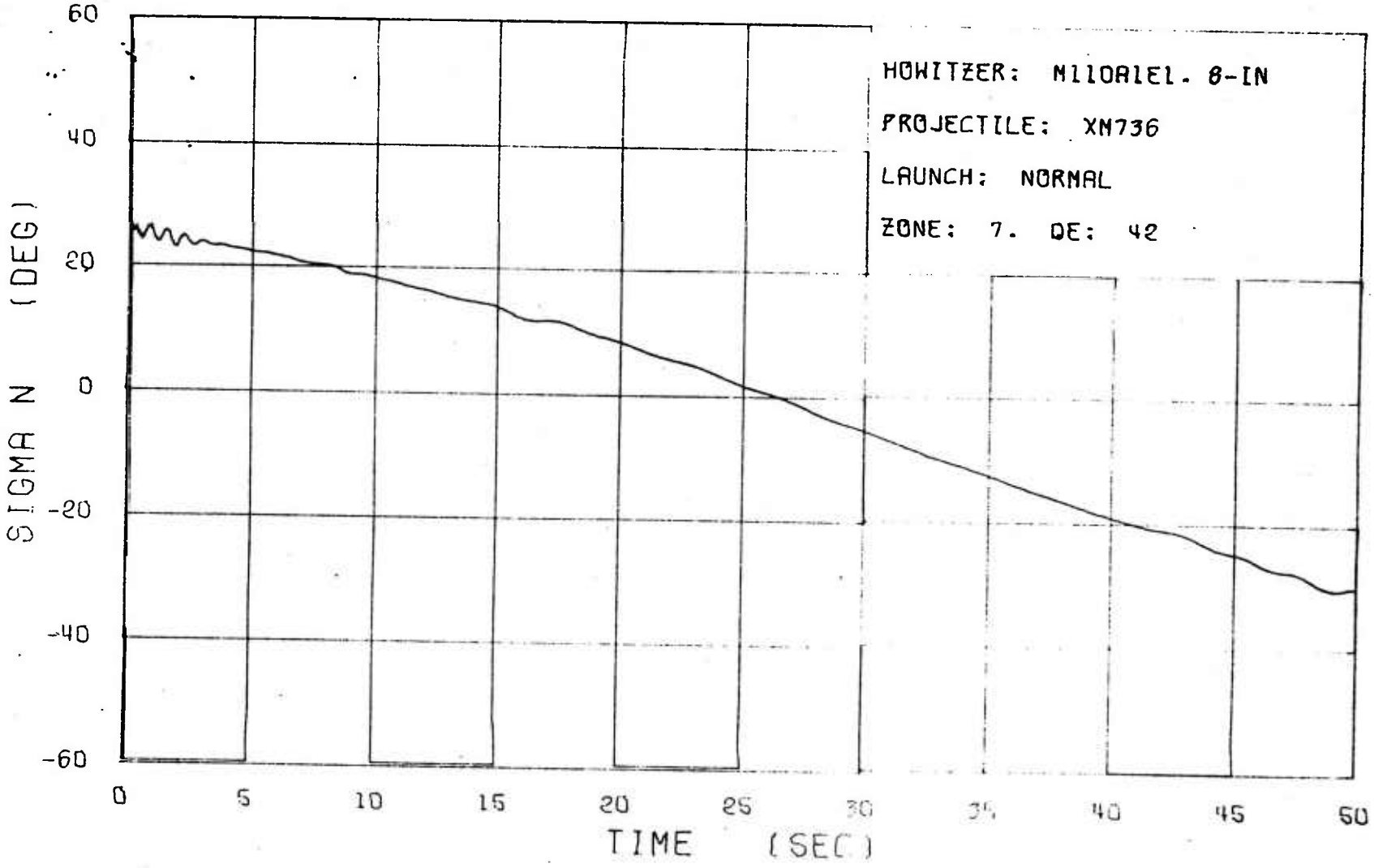

FIGURE 2. SIGMA N VS TIME ROUND 978

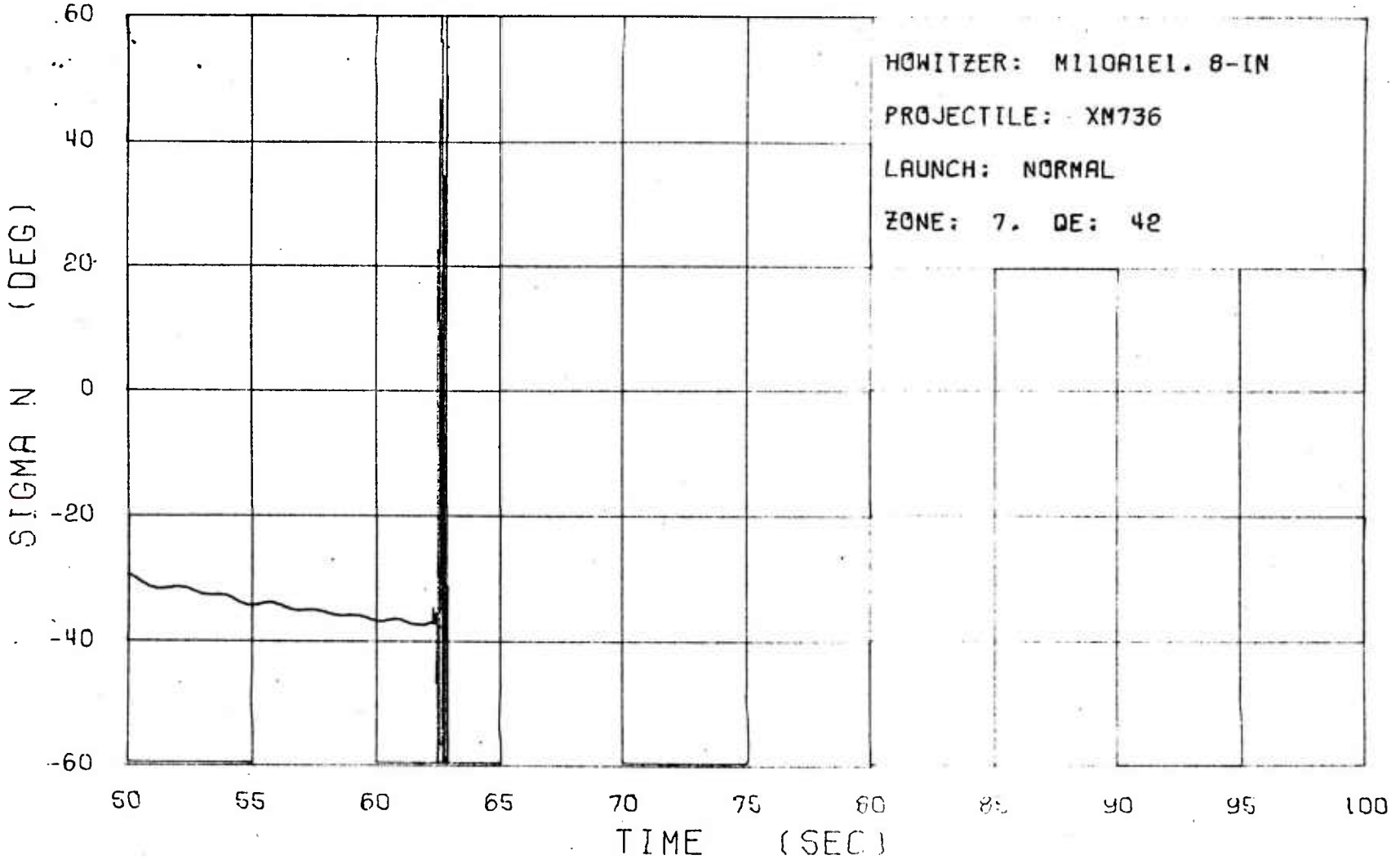

FIGURE 3. SIGMA N VS TIME ROUND 978

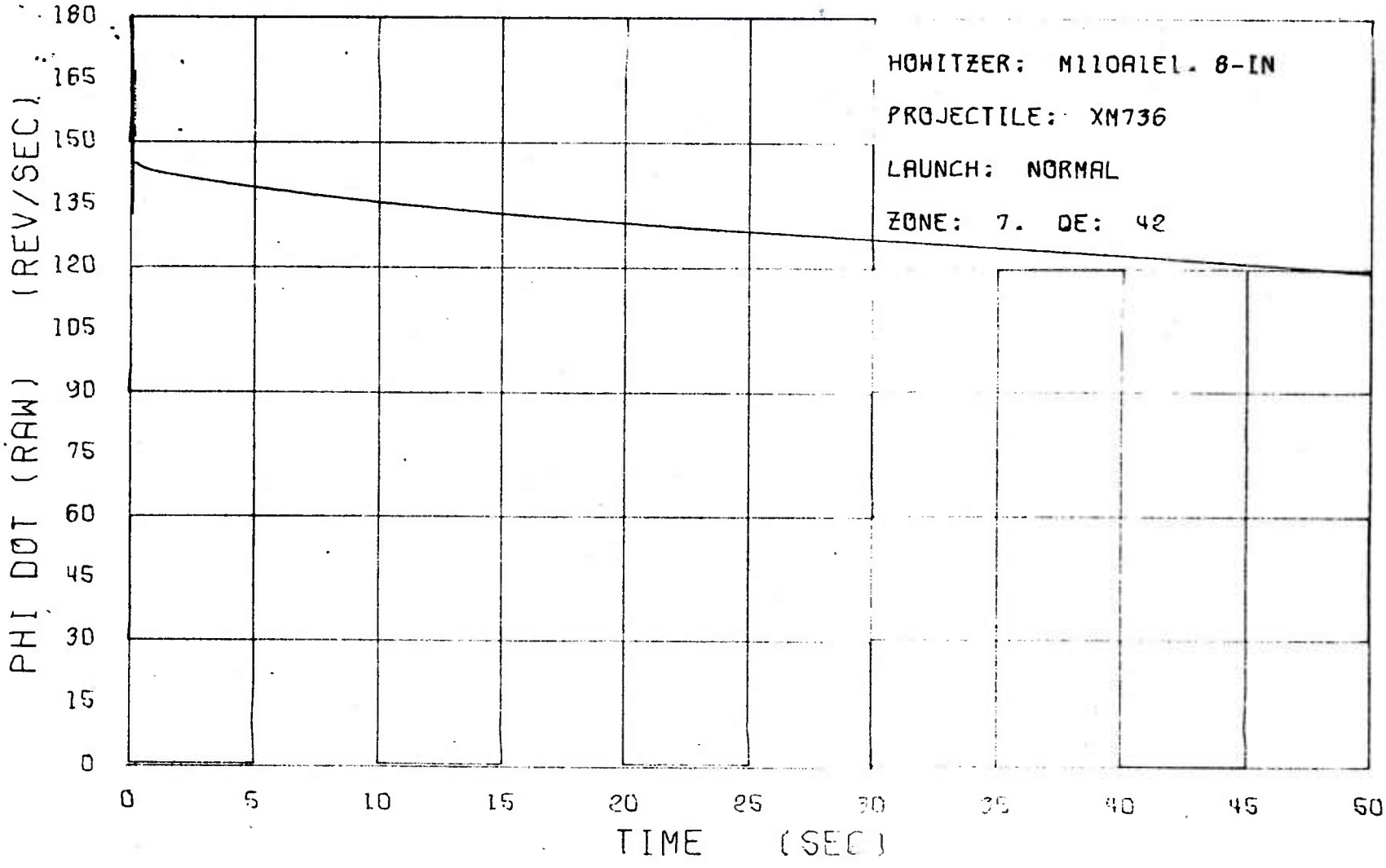

FIGURE 4. PHI DOT (RAW) VS TIME ROUND 978

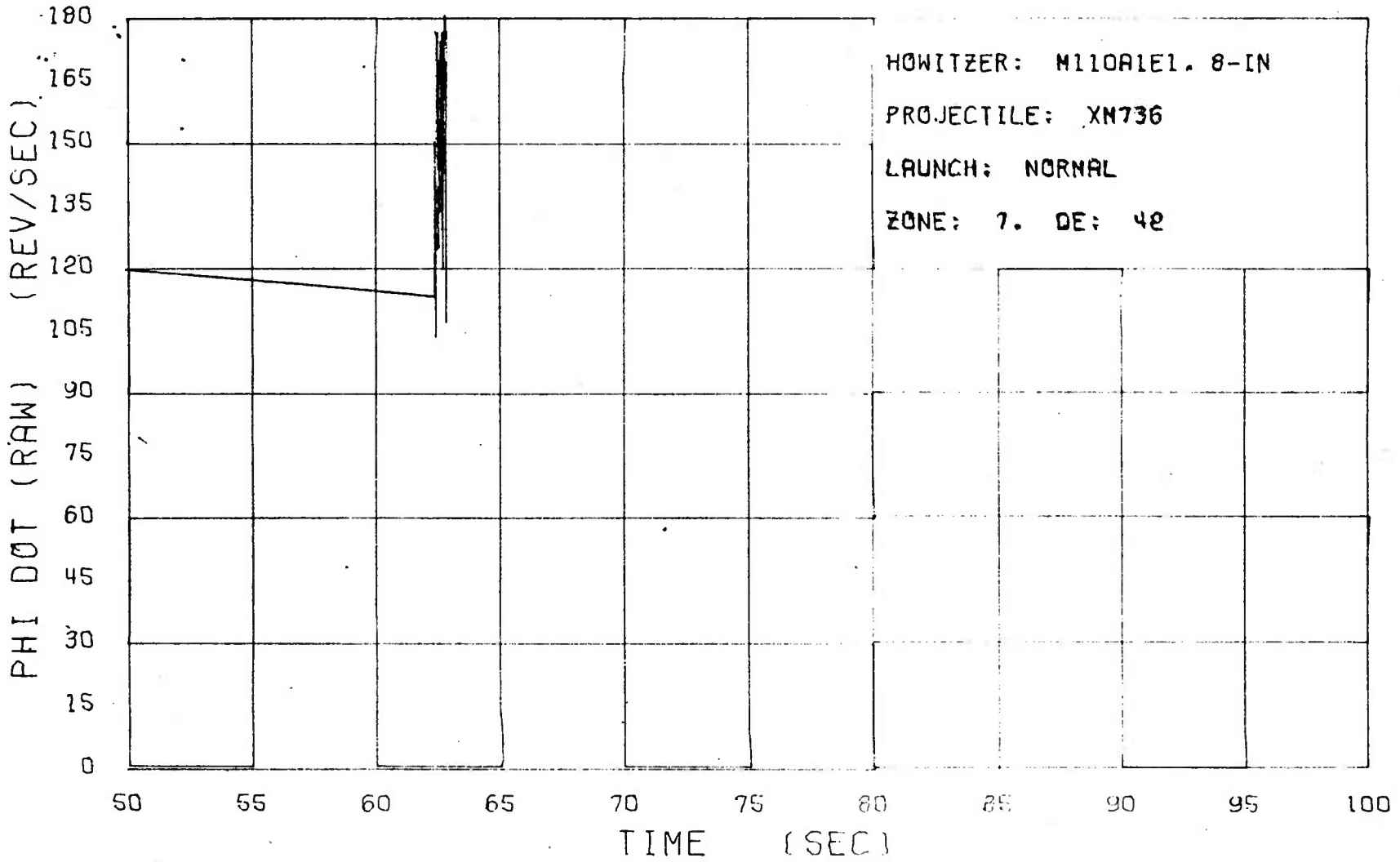

FIGURE 5. PHI DOT (RAW) VS TIME ROUND 978

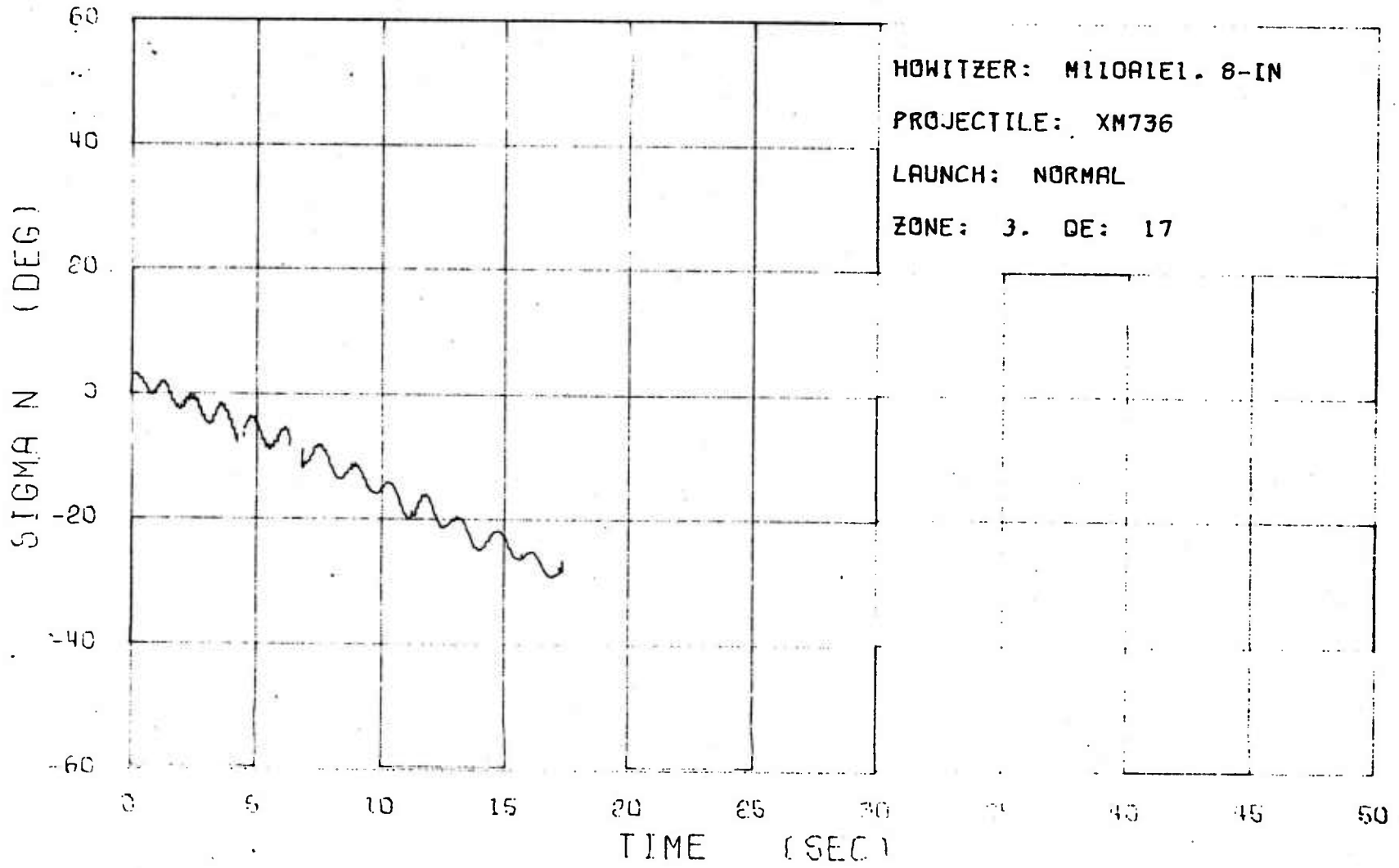

FIGURE 6. SIGMA N VS TIME ROUND 979

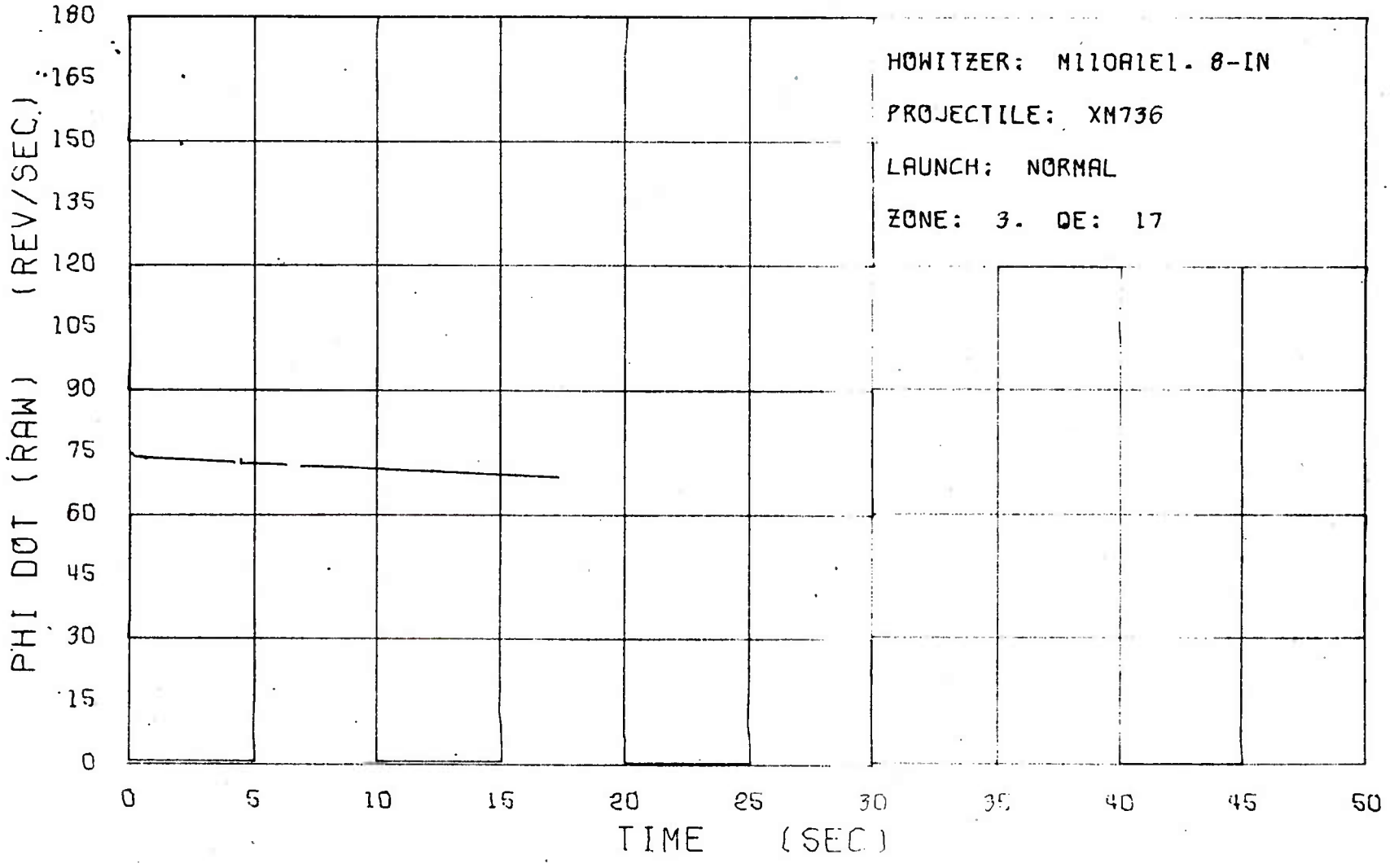

FIGURE 7. PHI DOT (RAW) VS TIME ROUND 979

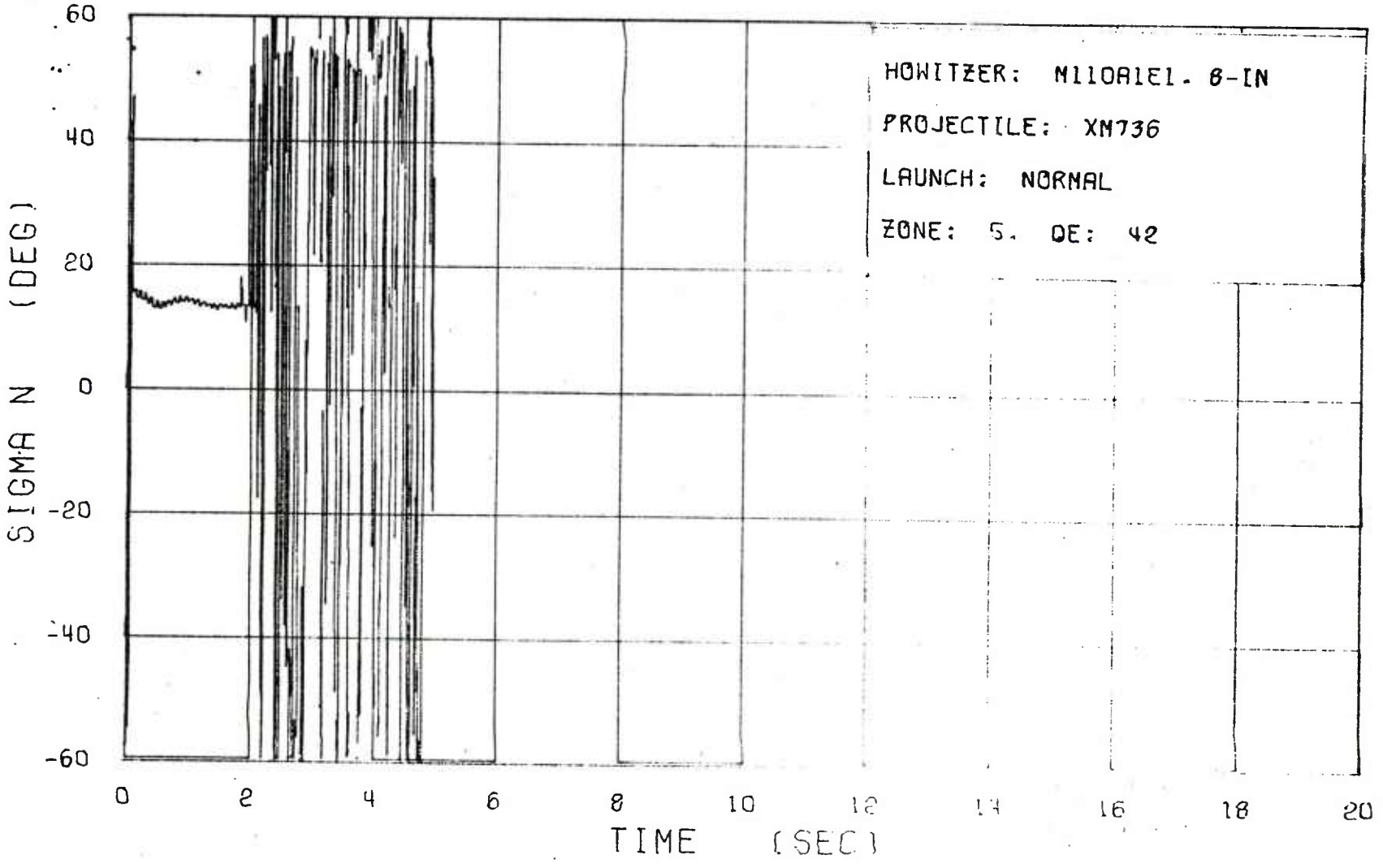

FIGURE 8. SIGMA N VS TIME ROUND 980

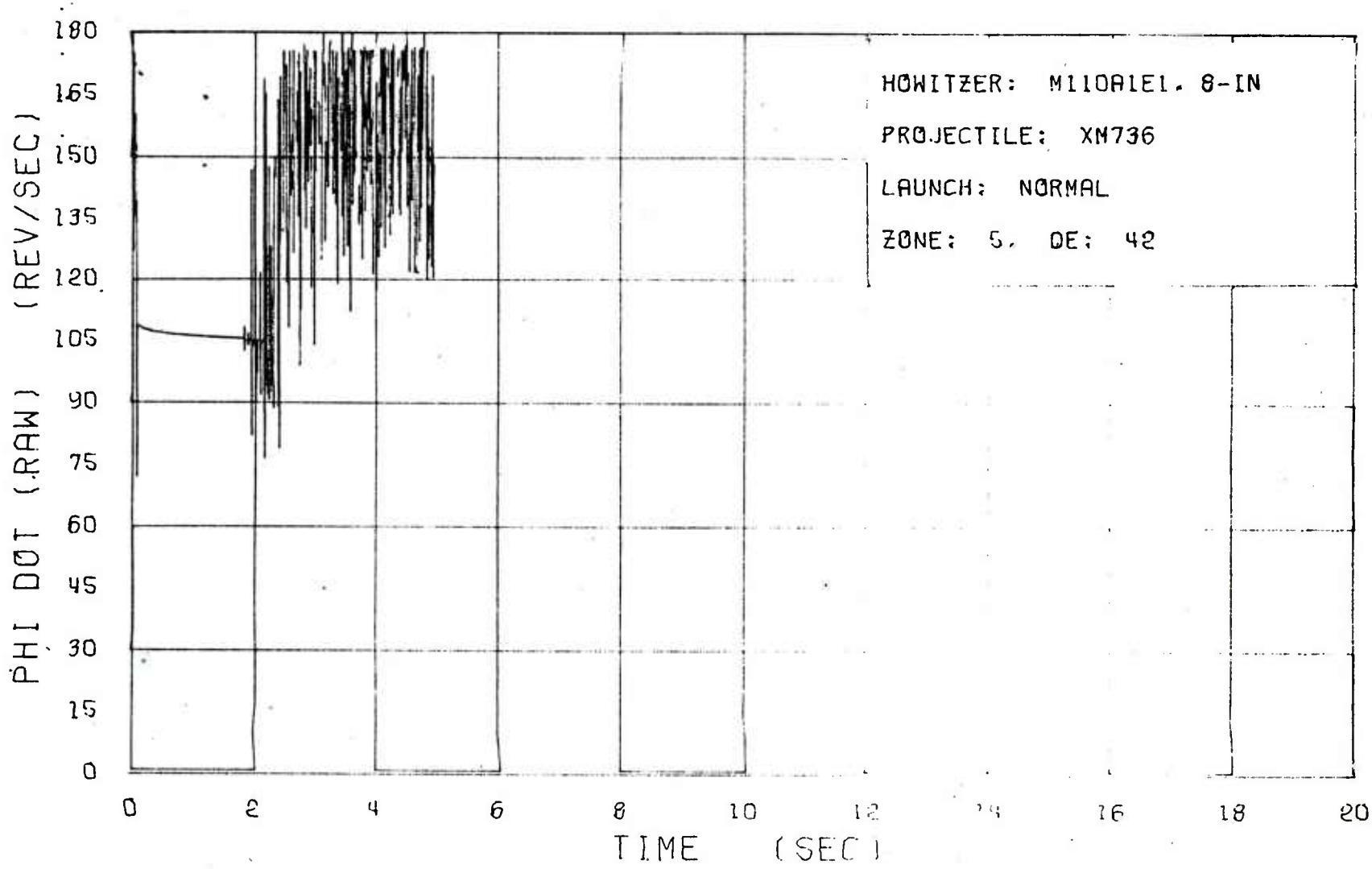

FIGURE 9. PHI DOT (RAW) VS TIME ROUND 080

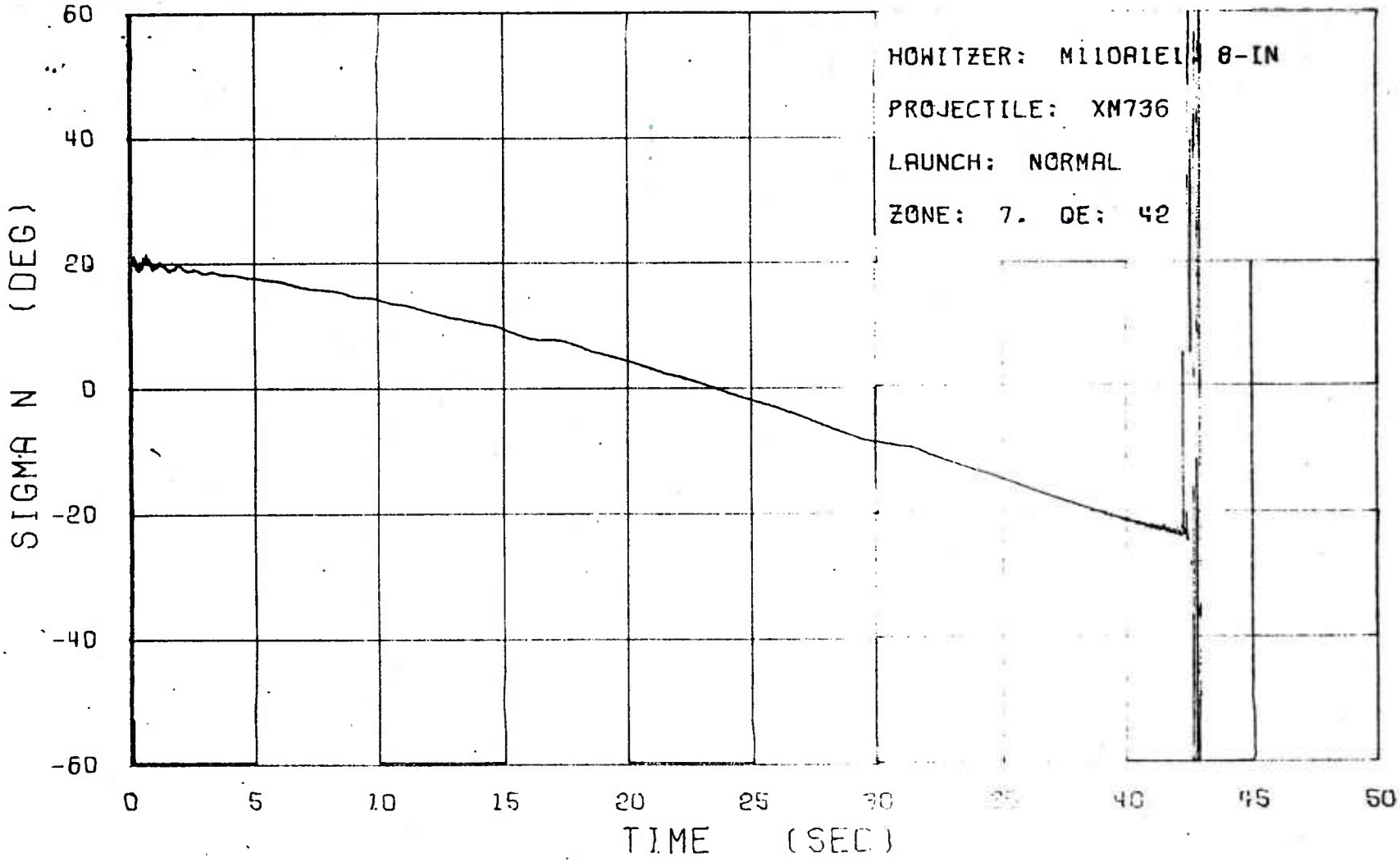

FIGURE 10. SIGMA N VS TIME ROUND 981

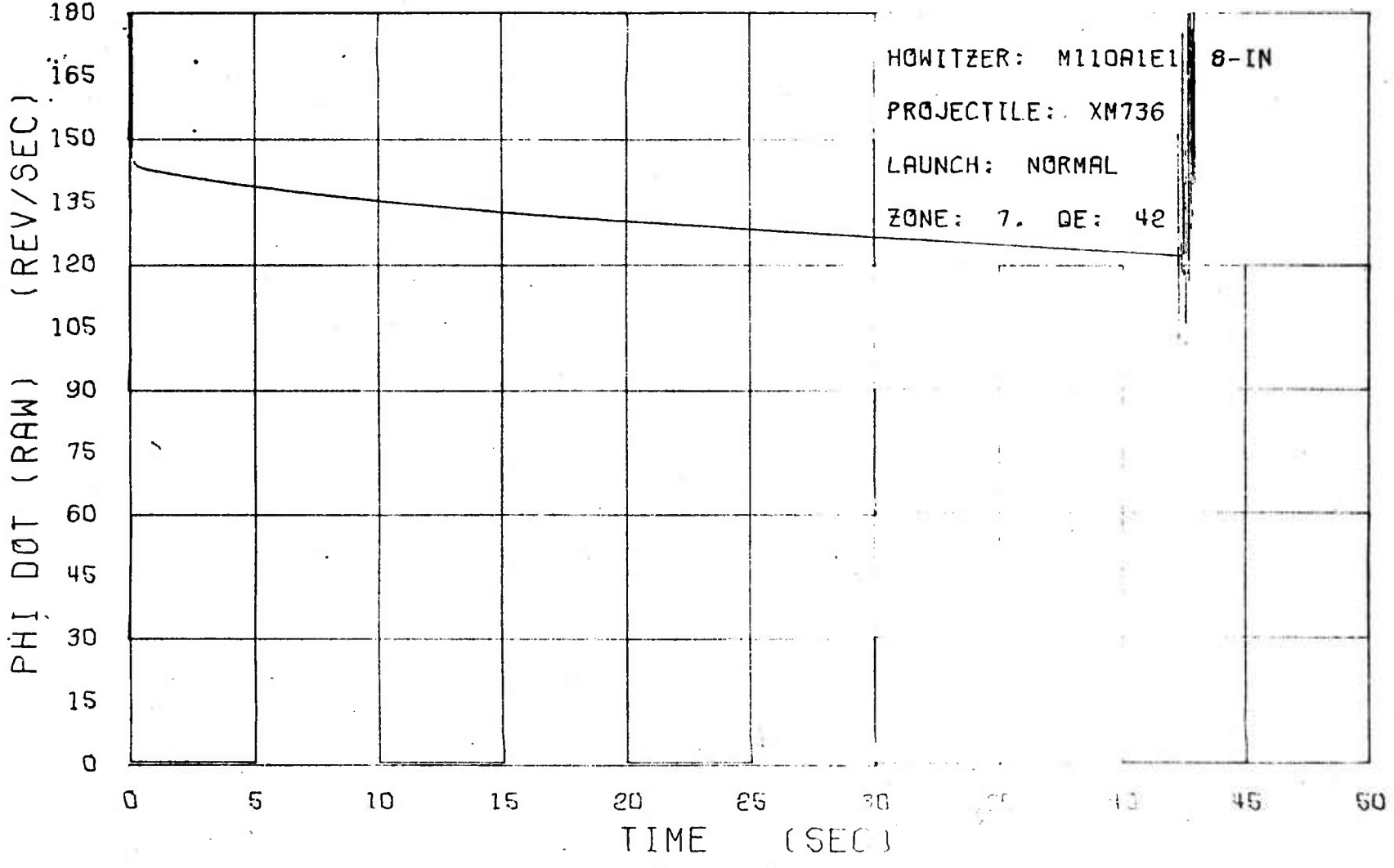

FIGURE 11. PHI DOT (RAW) VS TIME ROUND 981

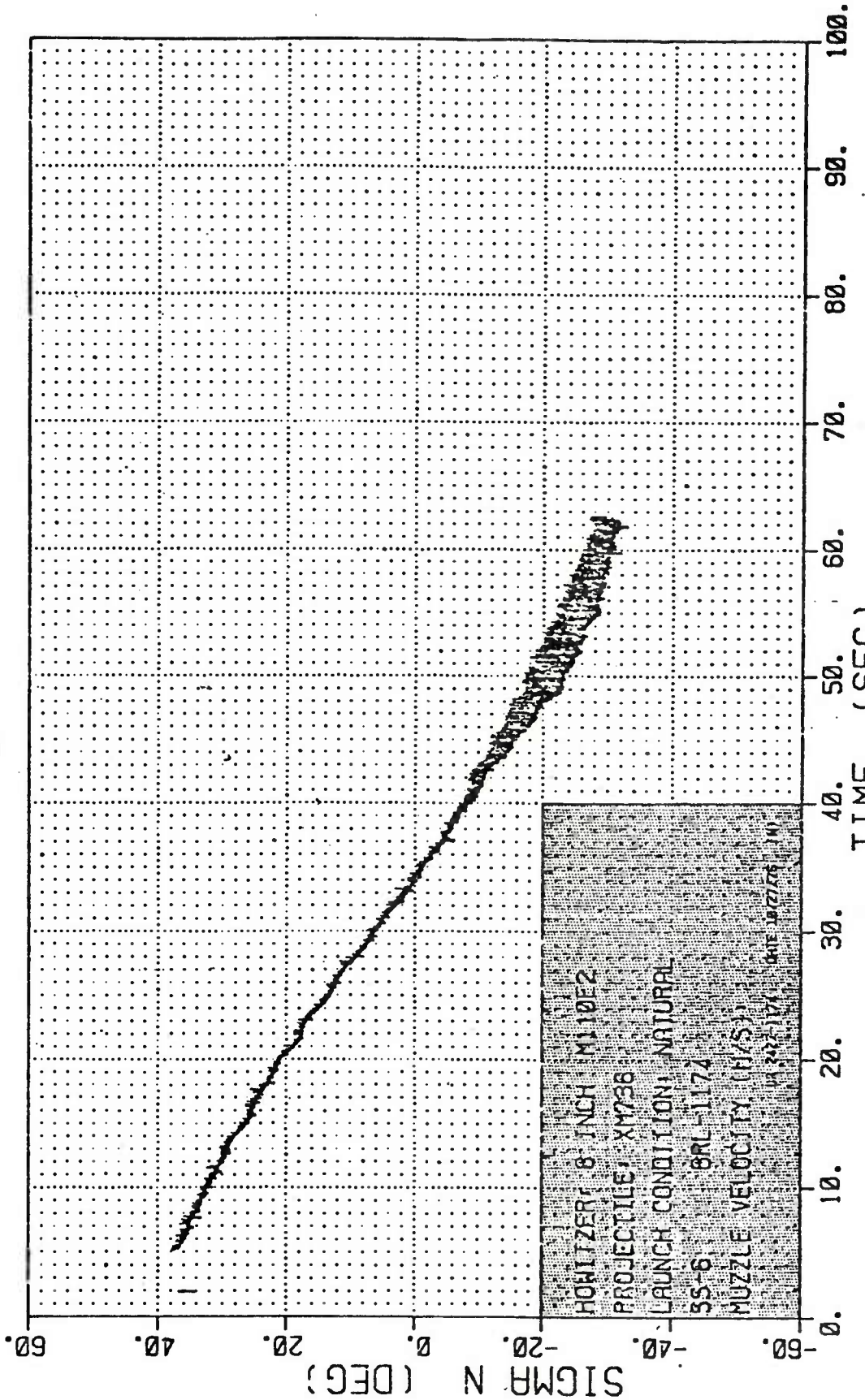

Figure 12. Sigma N versus Time - Round 1174

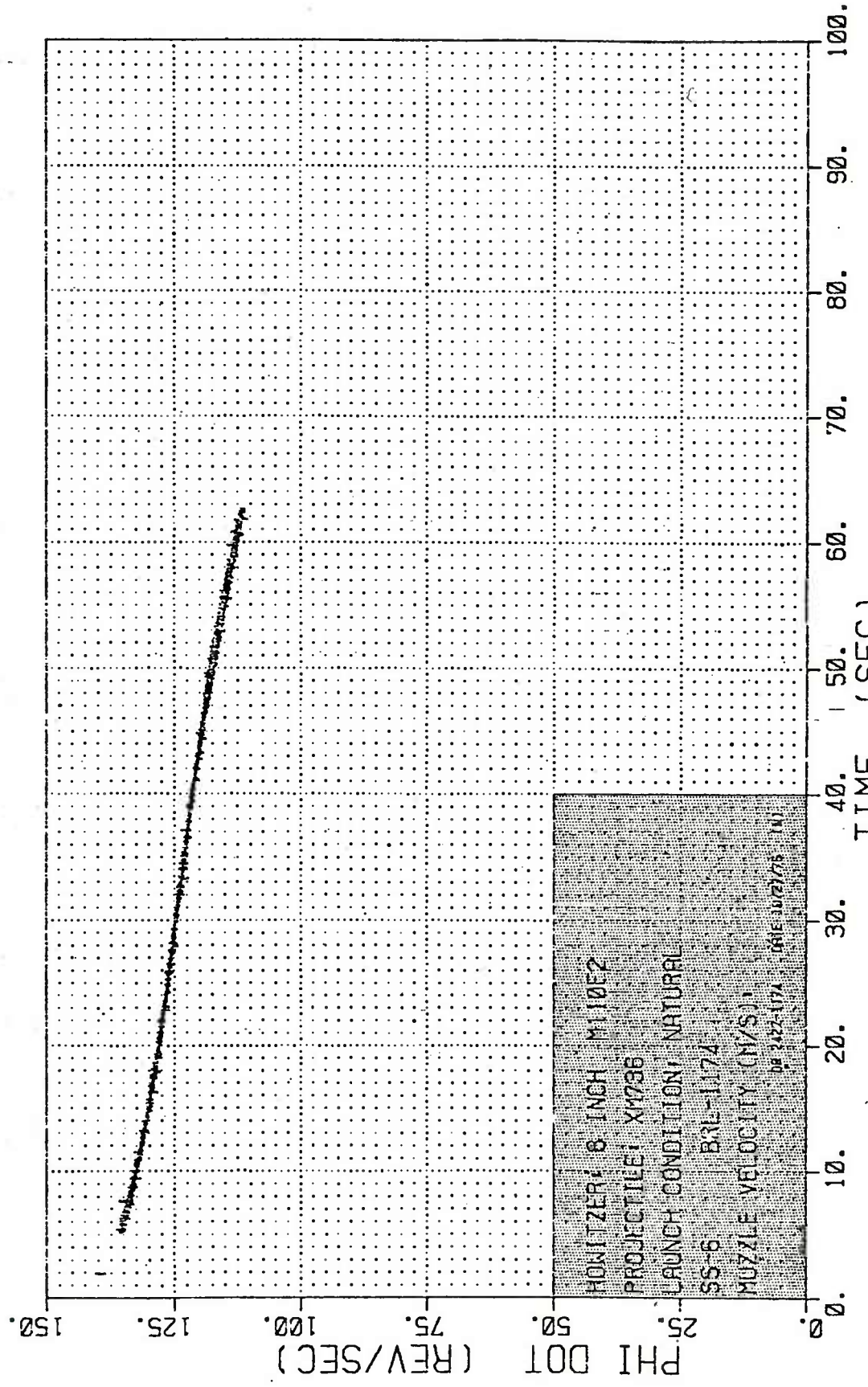

Figure 13. Phi Dot versus Time - Round 1174

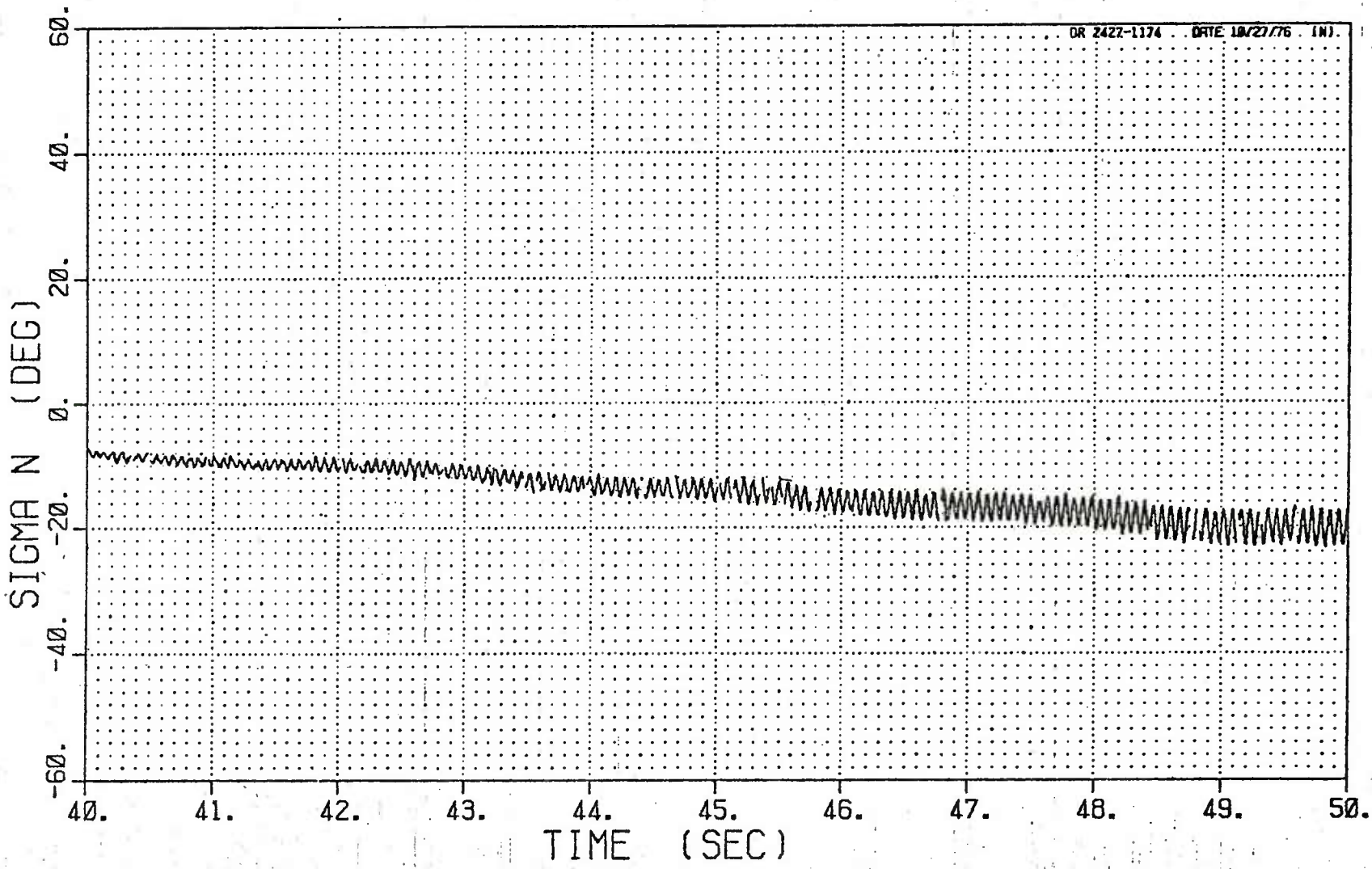

Figure 14. Sigma N versus Time - Round 1174 (40 - 50 seconds)

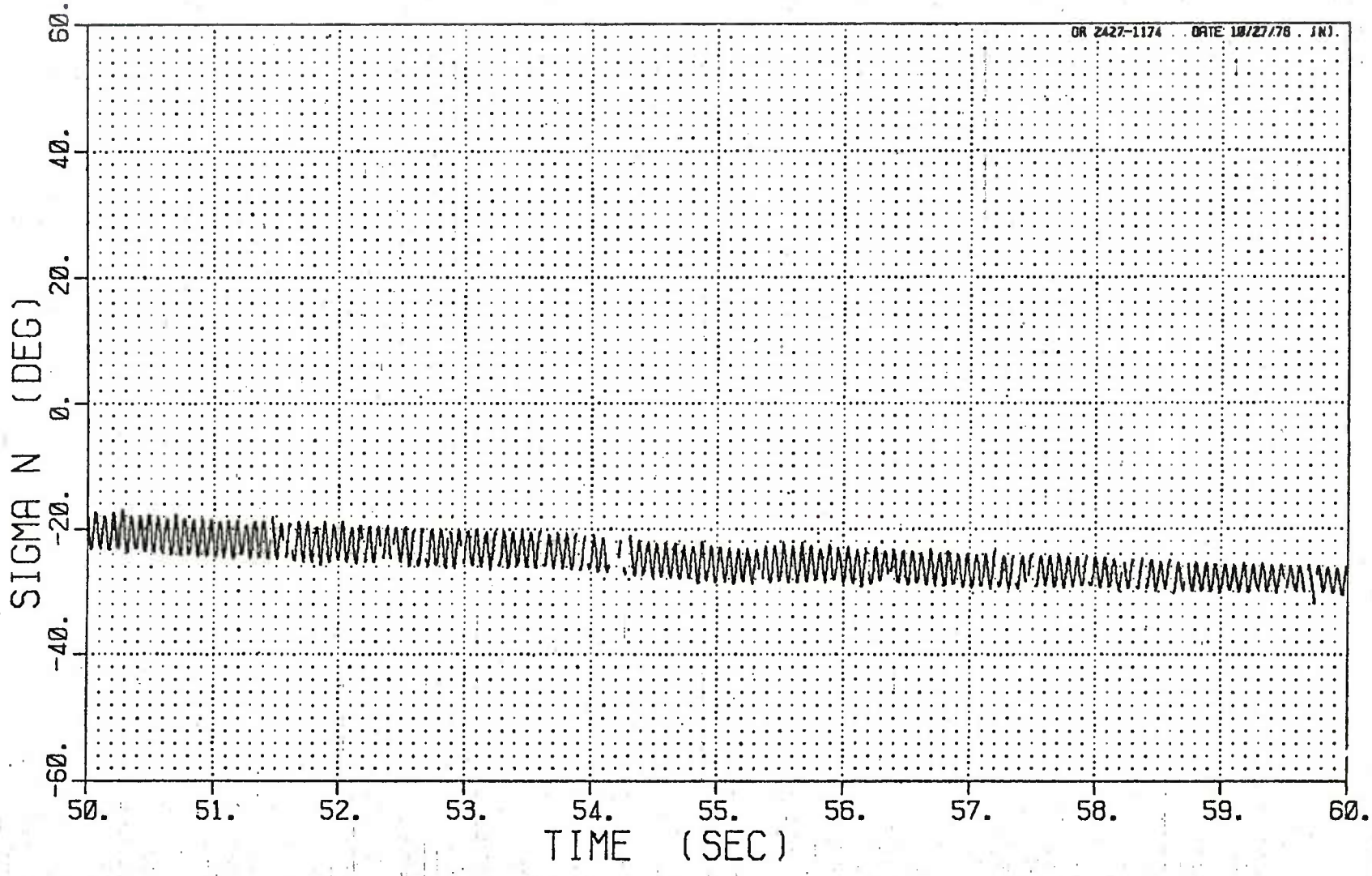

Figure 15. Sigma N versus Time - Round 1174 (50 - 60 seconds)

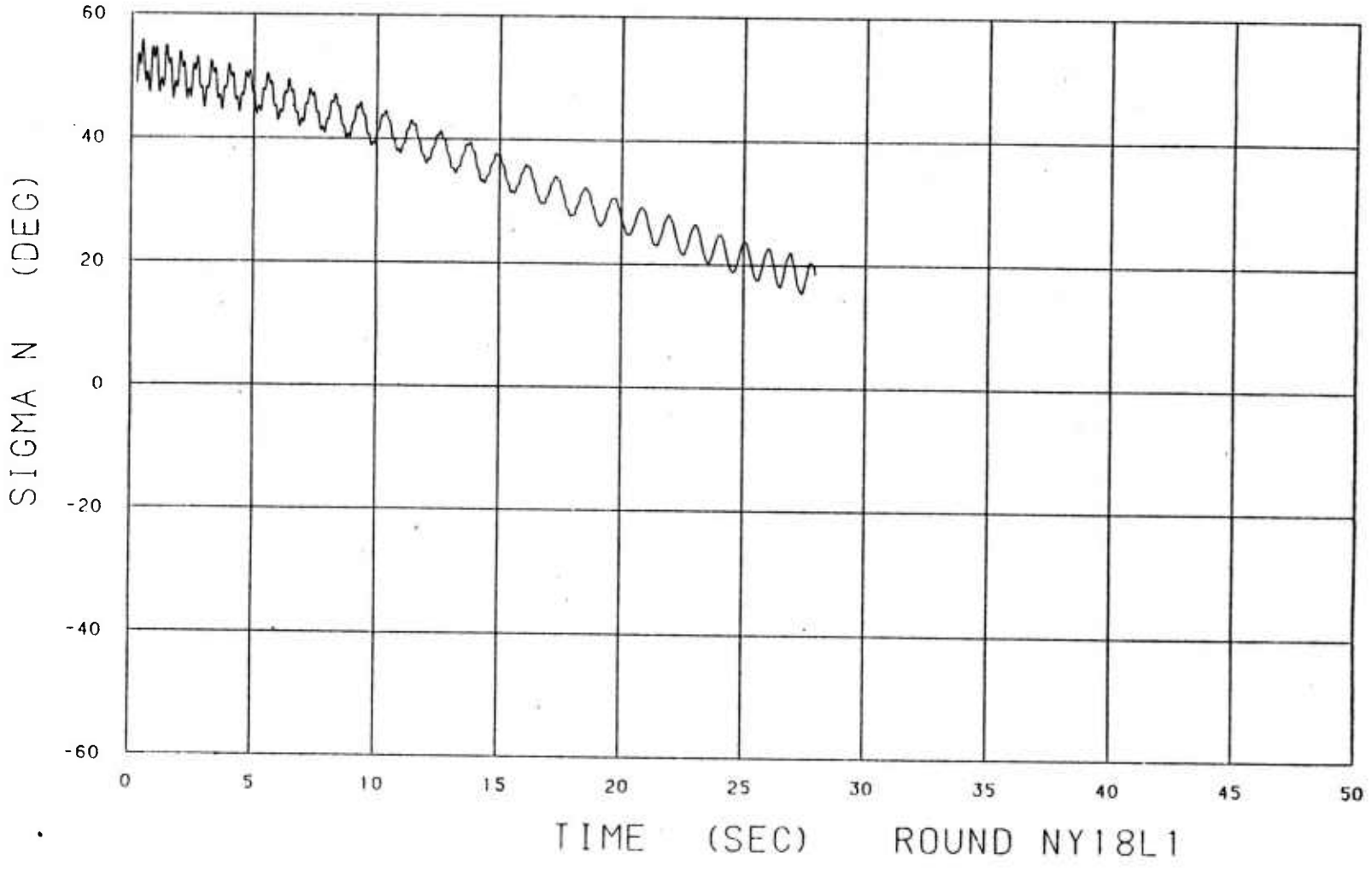

Figure 16. Sigma N versus Time for Round NY18L1.

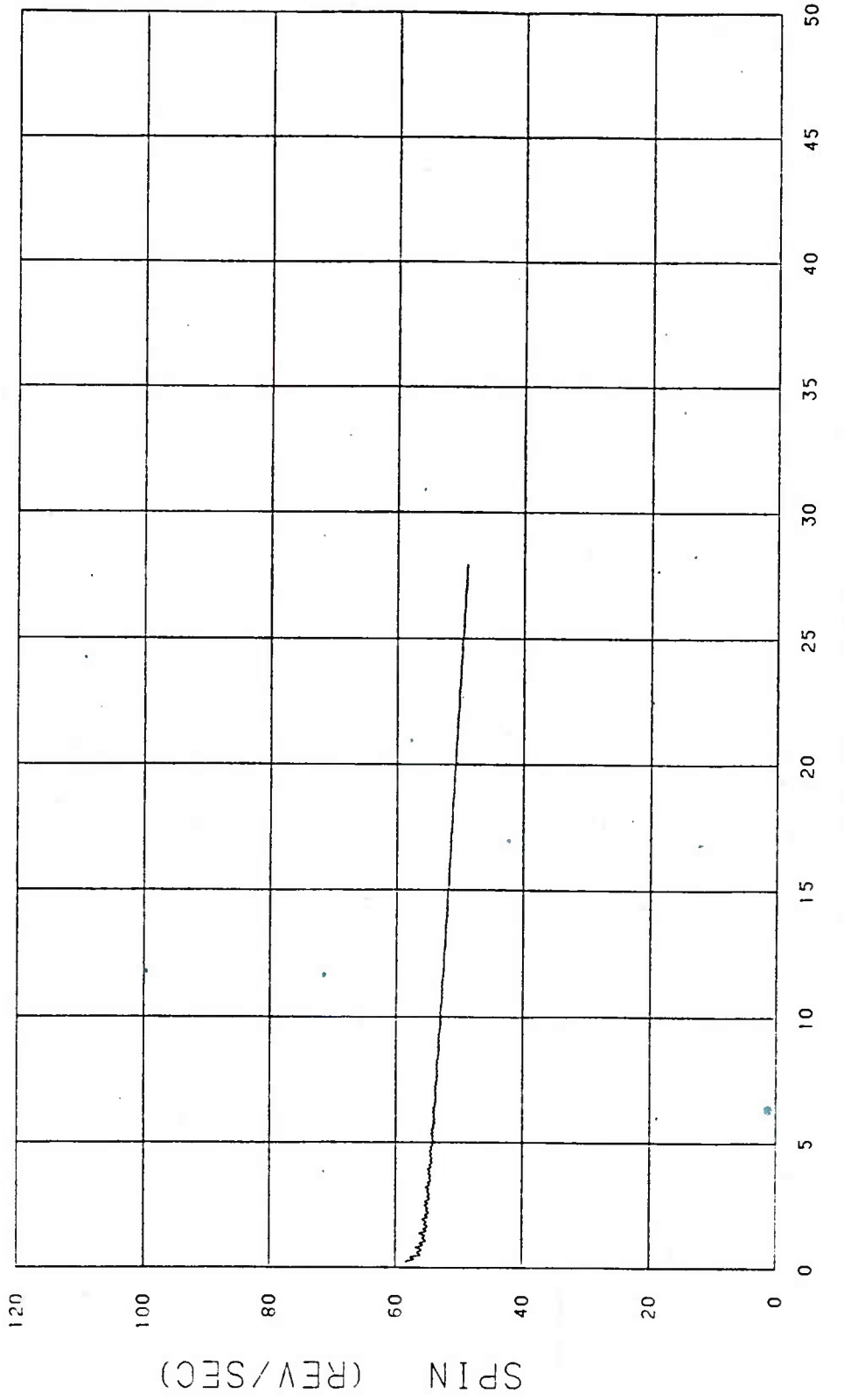

Figure 17. Spin versus Time for Round NY18L1.

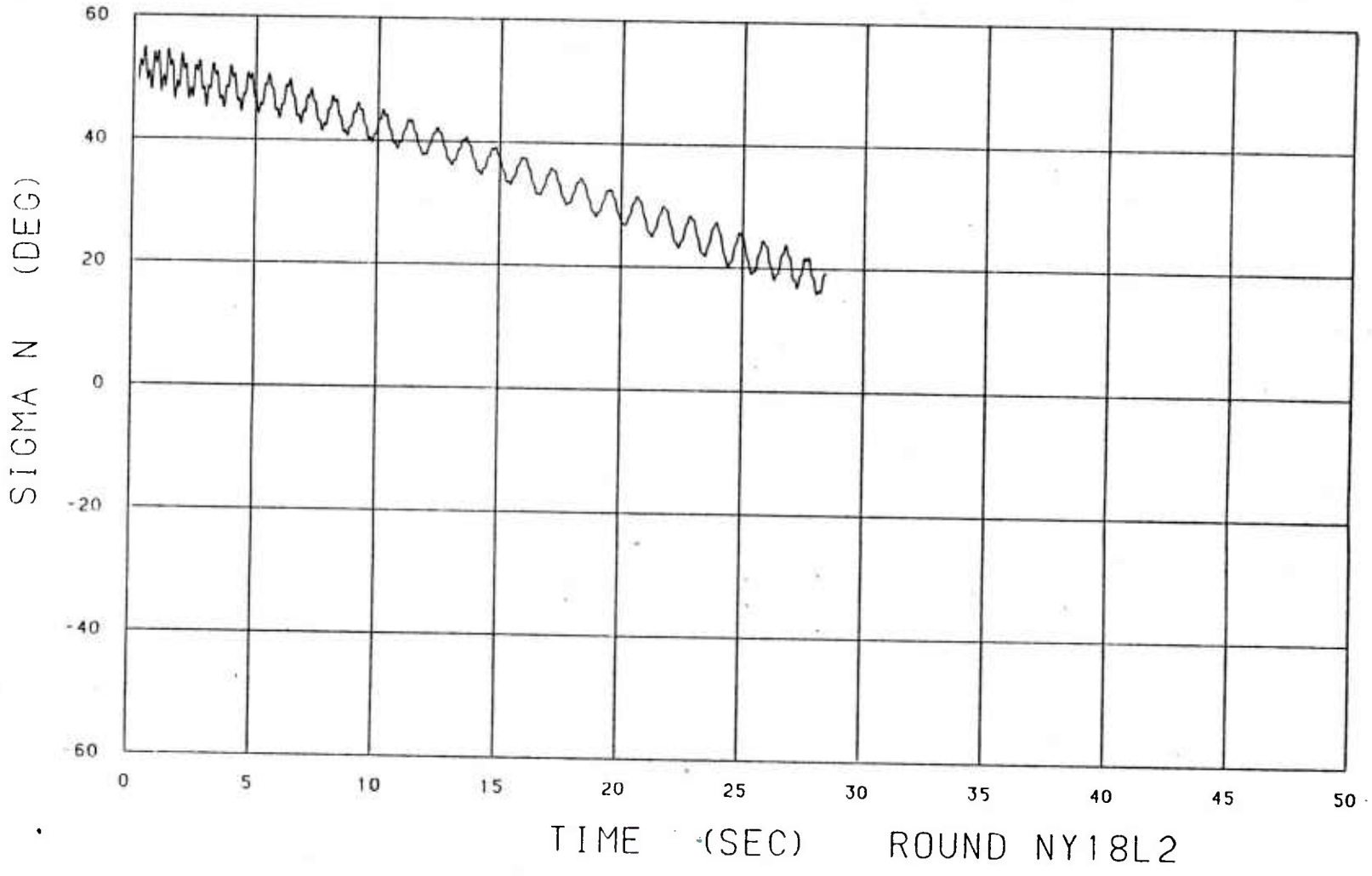

Figure 18. Sigma N versus Time for Round NY18L2.

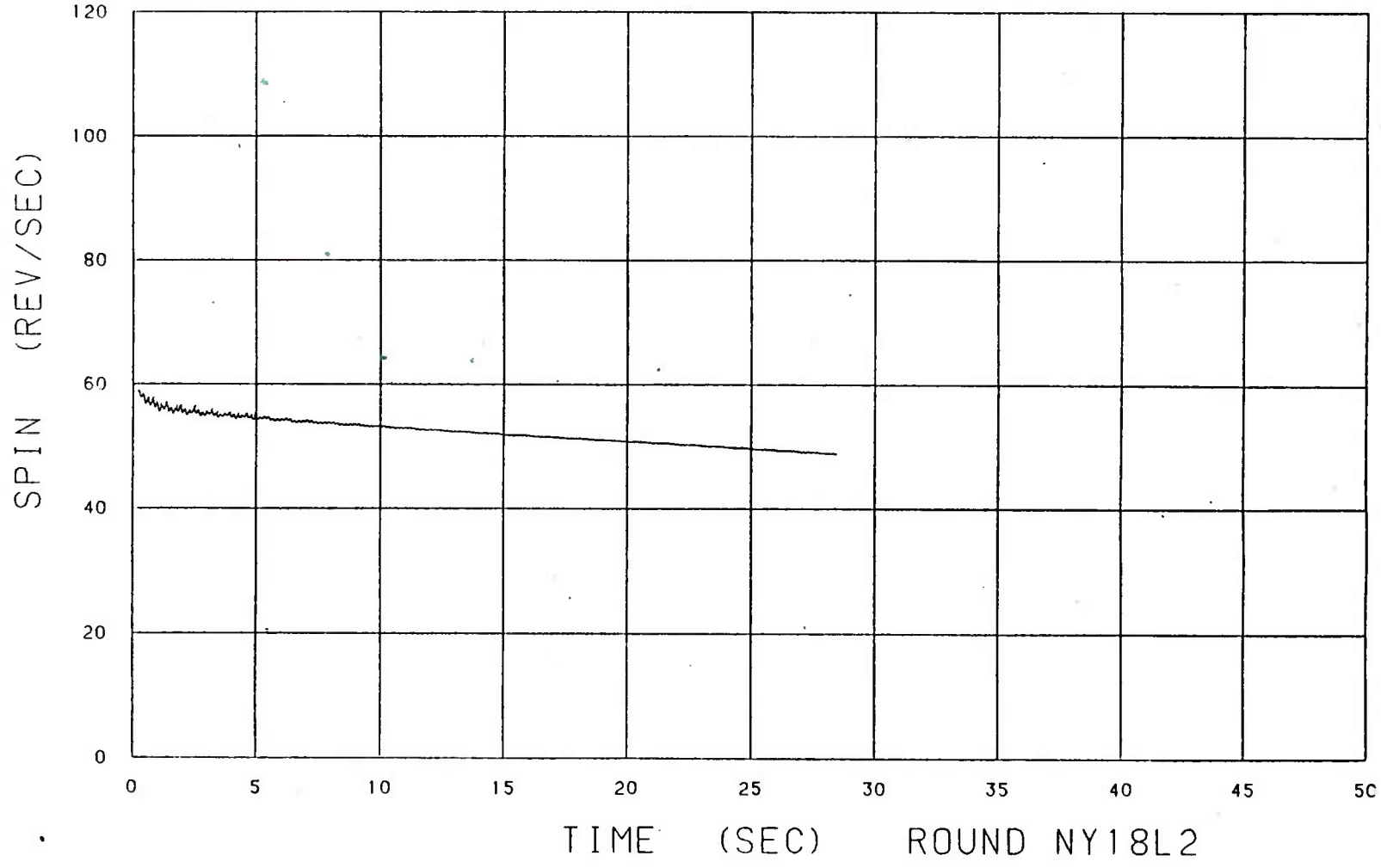

Figure 19. Spin versus Time for Round NY18L2.

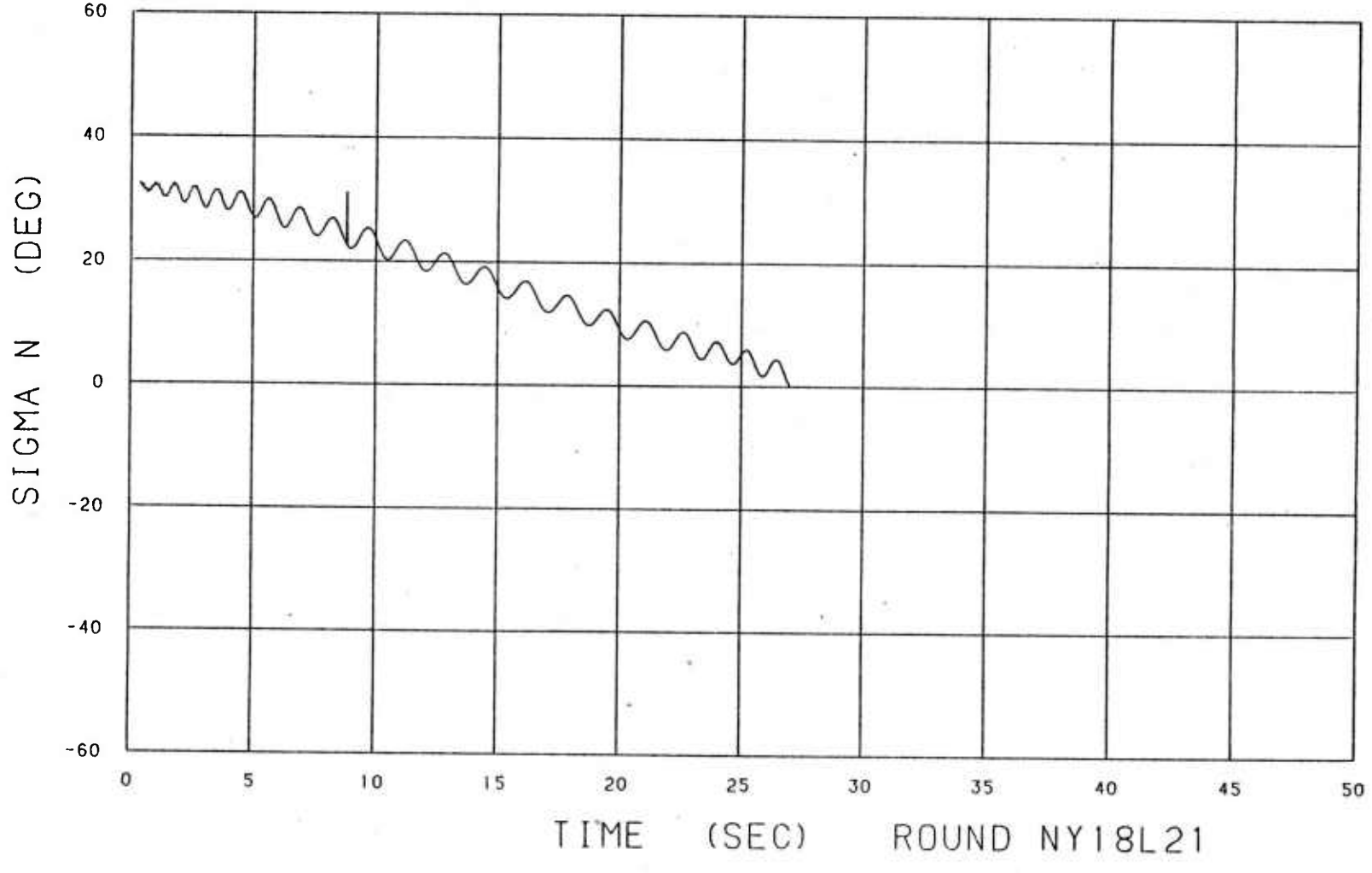

Figure 20. Sigma N versus Time for Round NY18L21.

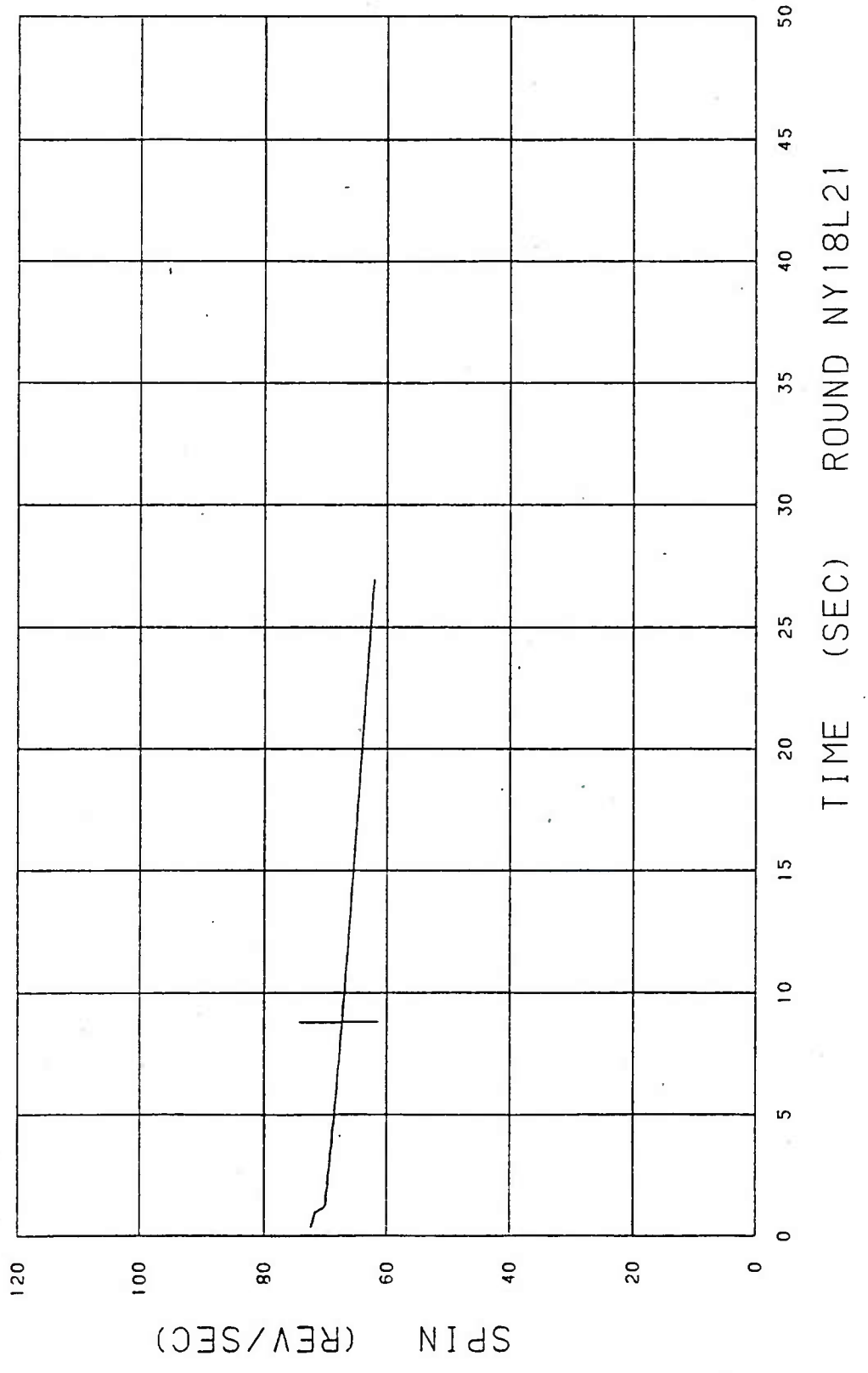

Figure 21. Spin versus Time for Round NY18L21.

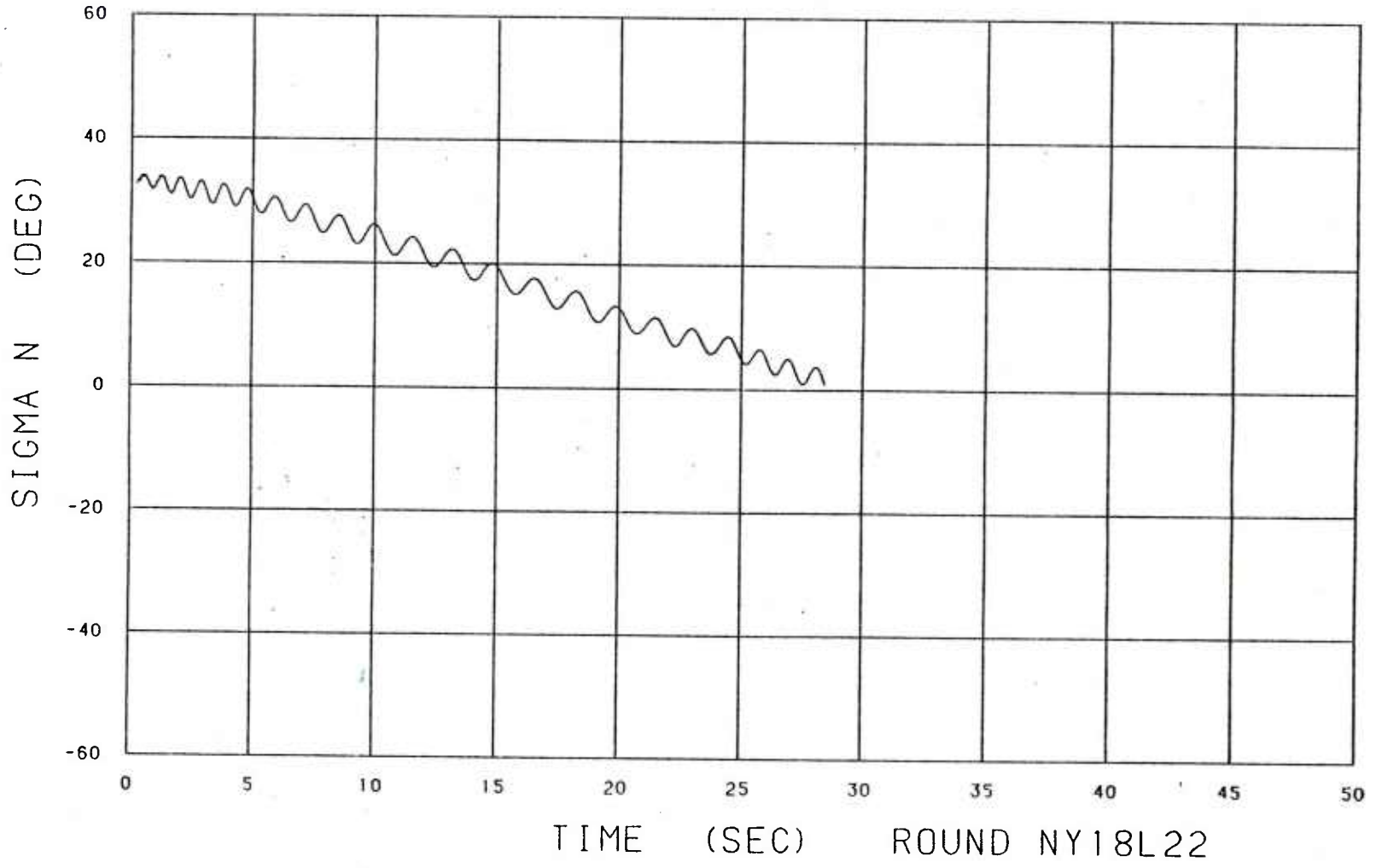

Figure 22. Sigma N versus Time for Round NY18L22.

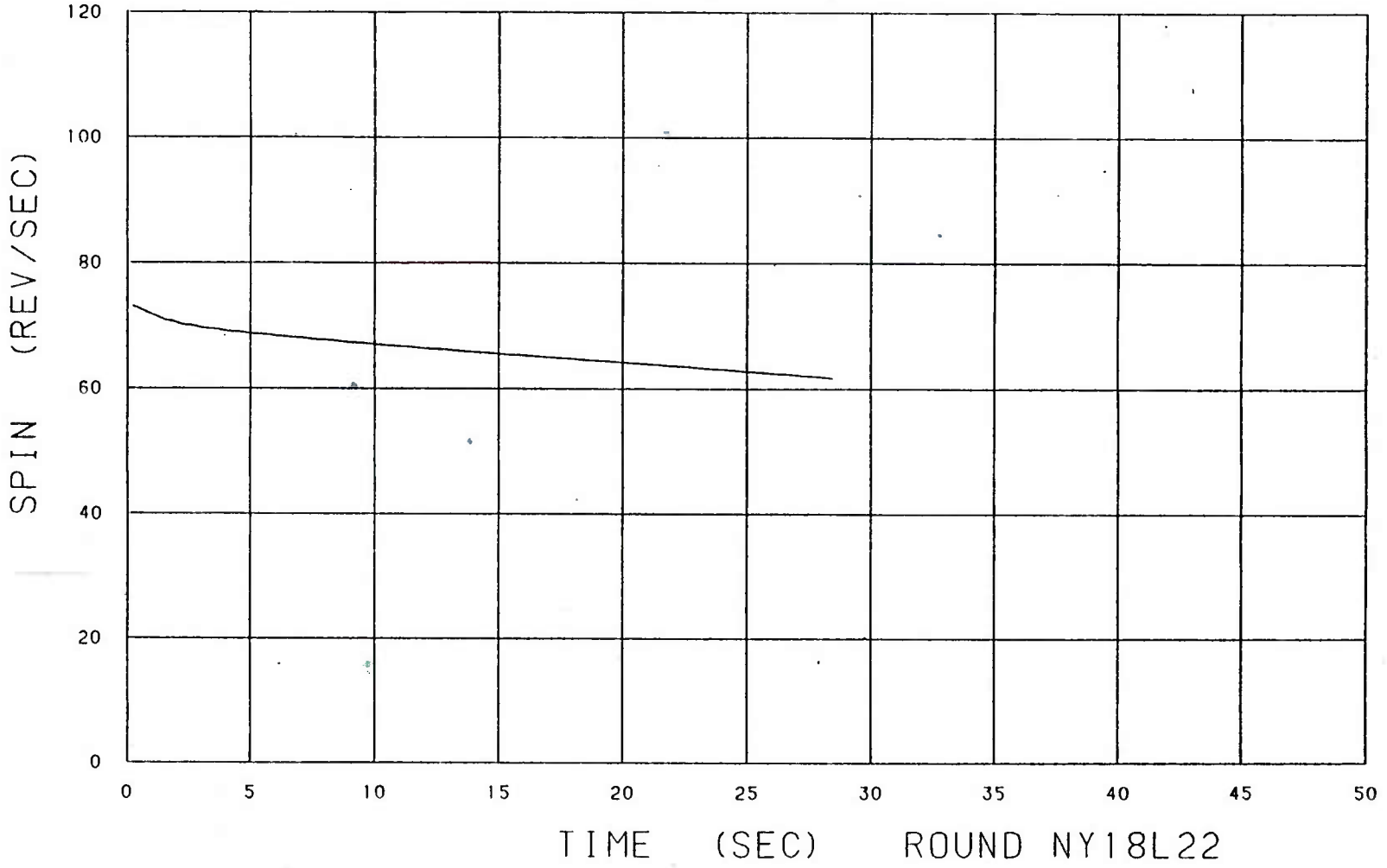

Figure 23. Spin versus Time for Round NY18L22.

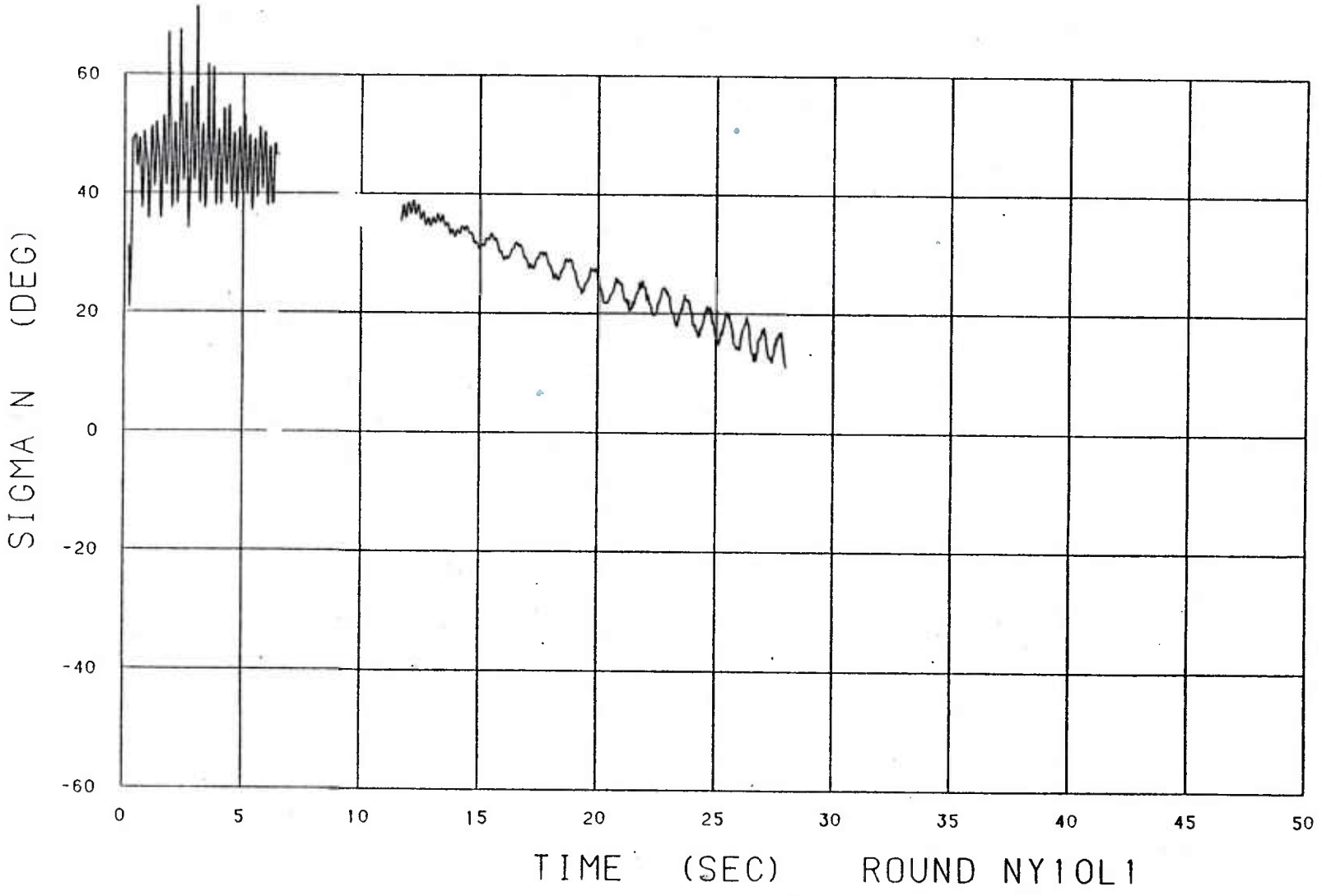

Figure 24. Sigma N versus Time for Round NY10L1.

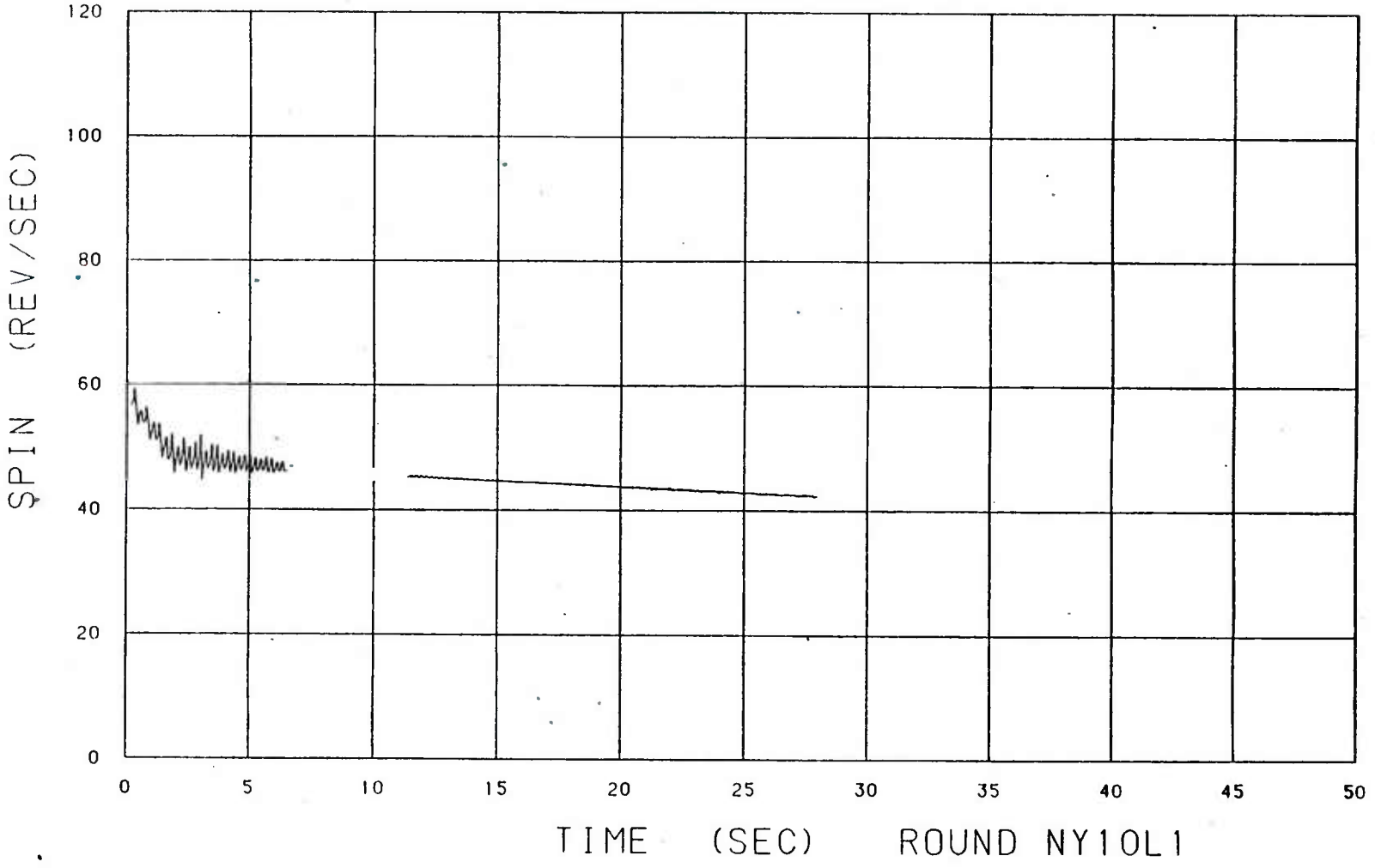

Figure 25. Spin versus Time for Round NY10L1.

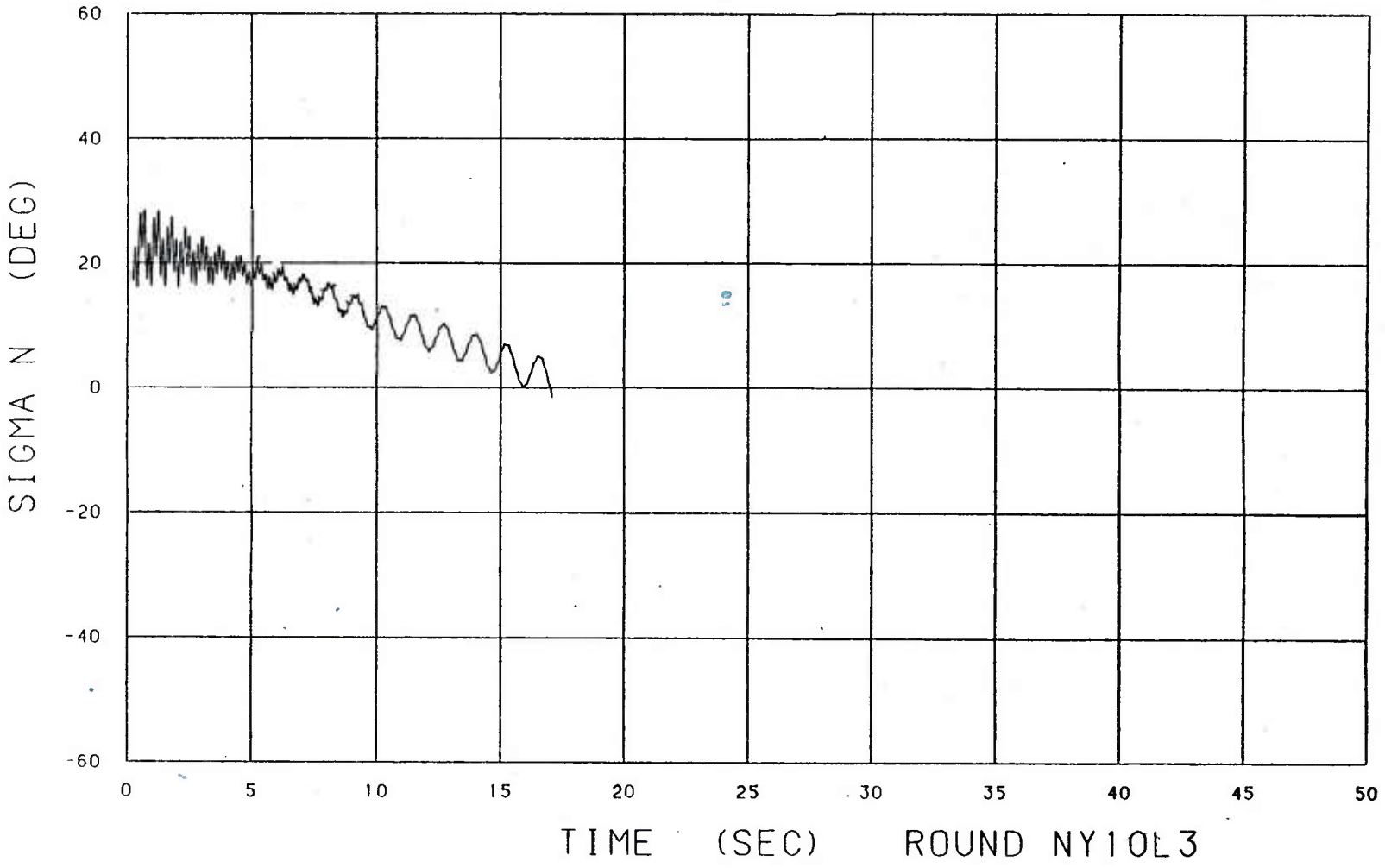

Figure 26. Sigma N versus Time for Round NY10L3.

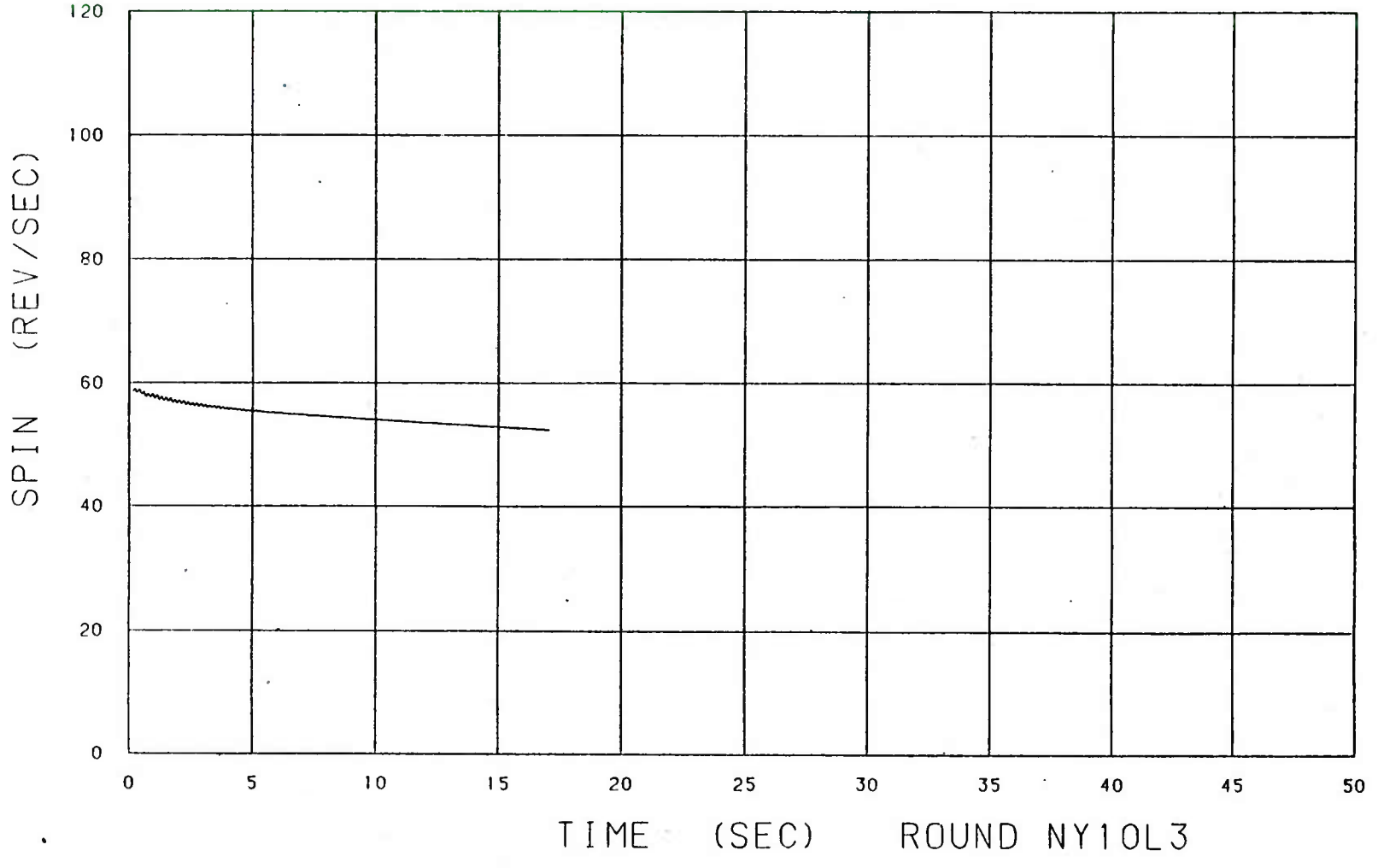

Figure 27. Spin versus Time for Round NY10L3.

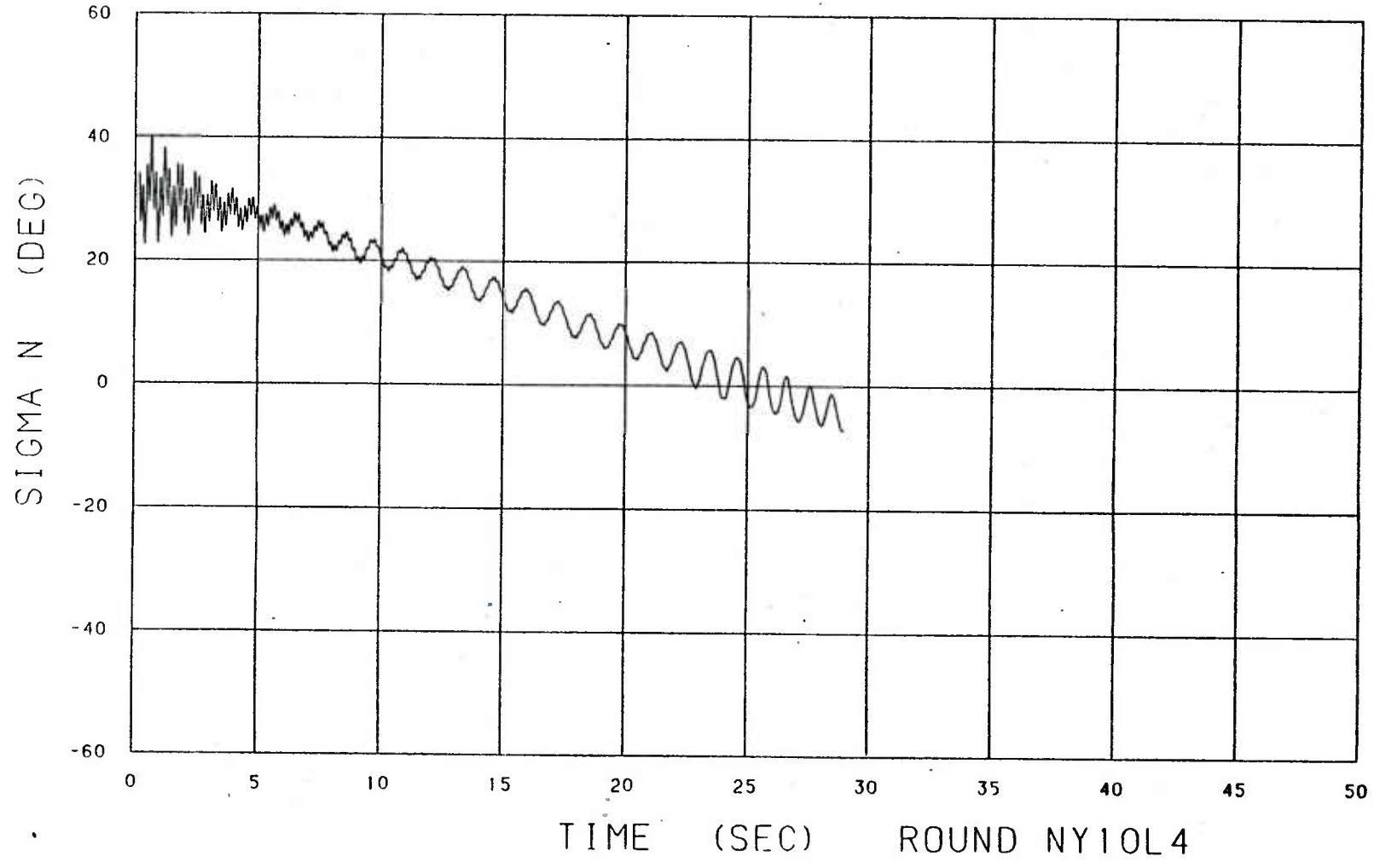

Figure 28. Sigma N versus Time for Round NY10L4.

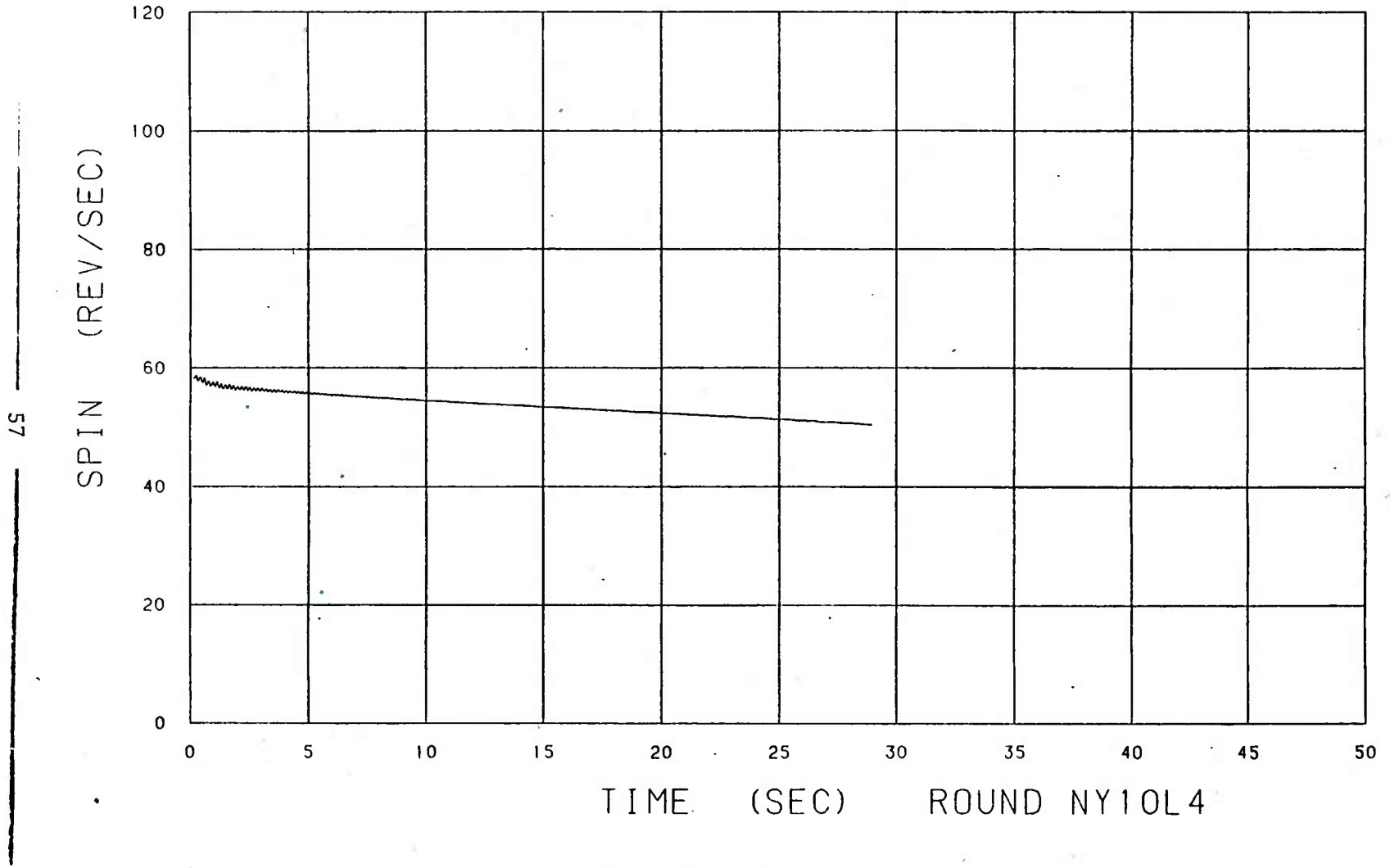

Figure 29.. Spin versus Time for Round NY10L4.

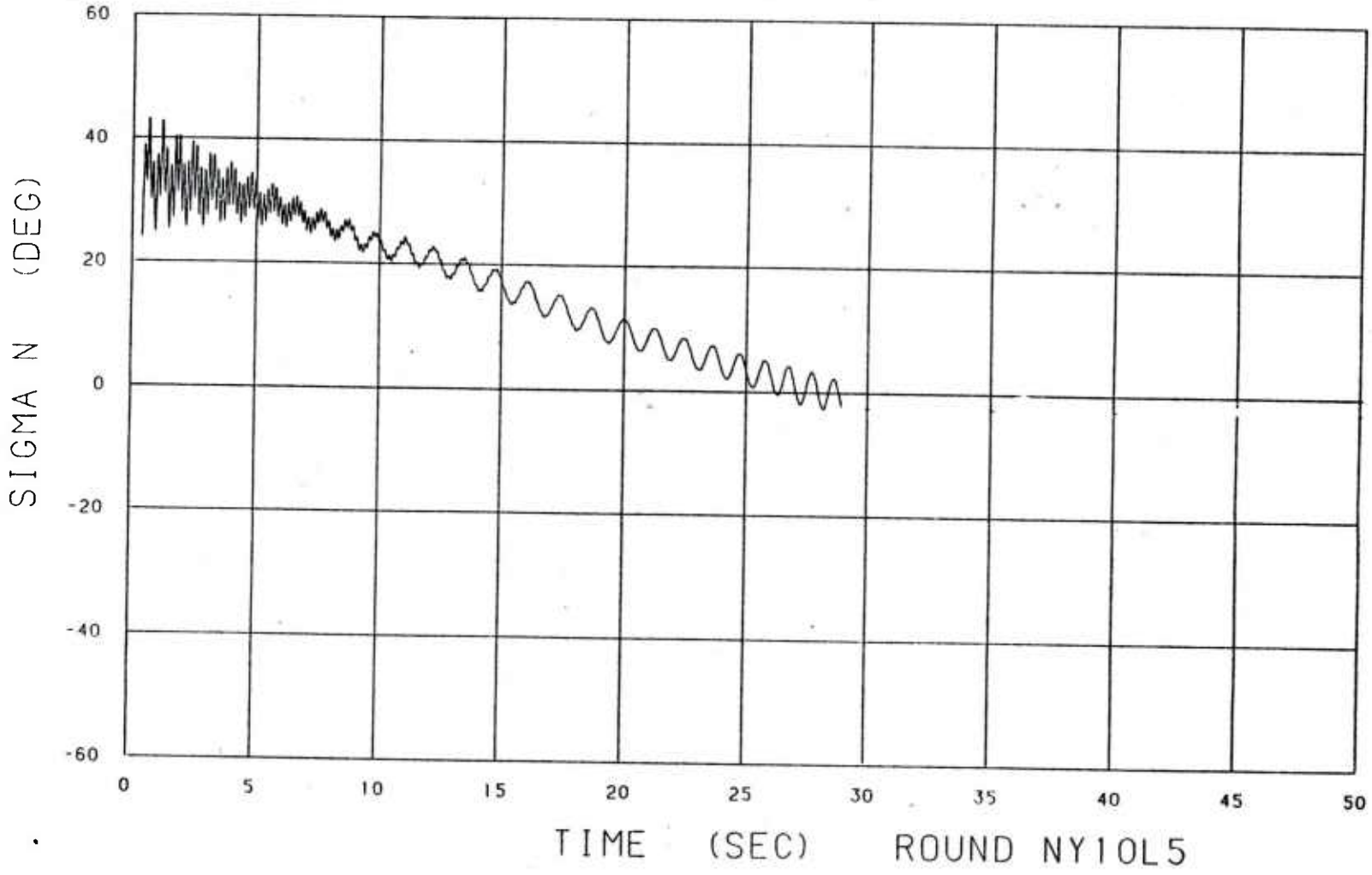

Figure 30. Sigma N versus Time for Round NY10L5.

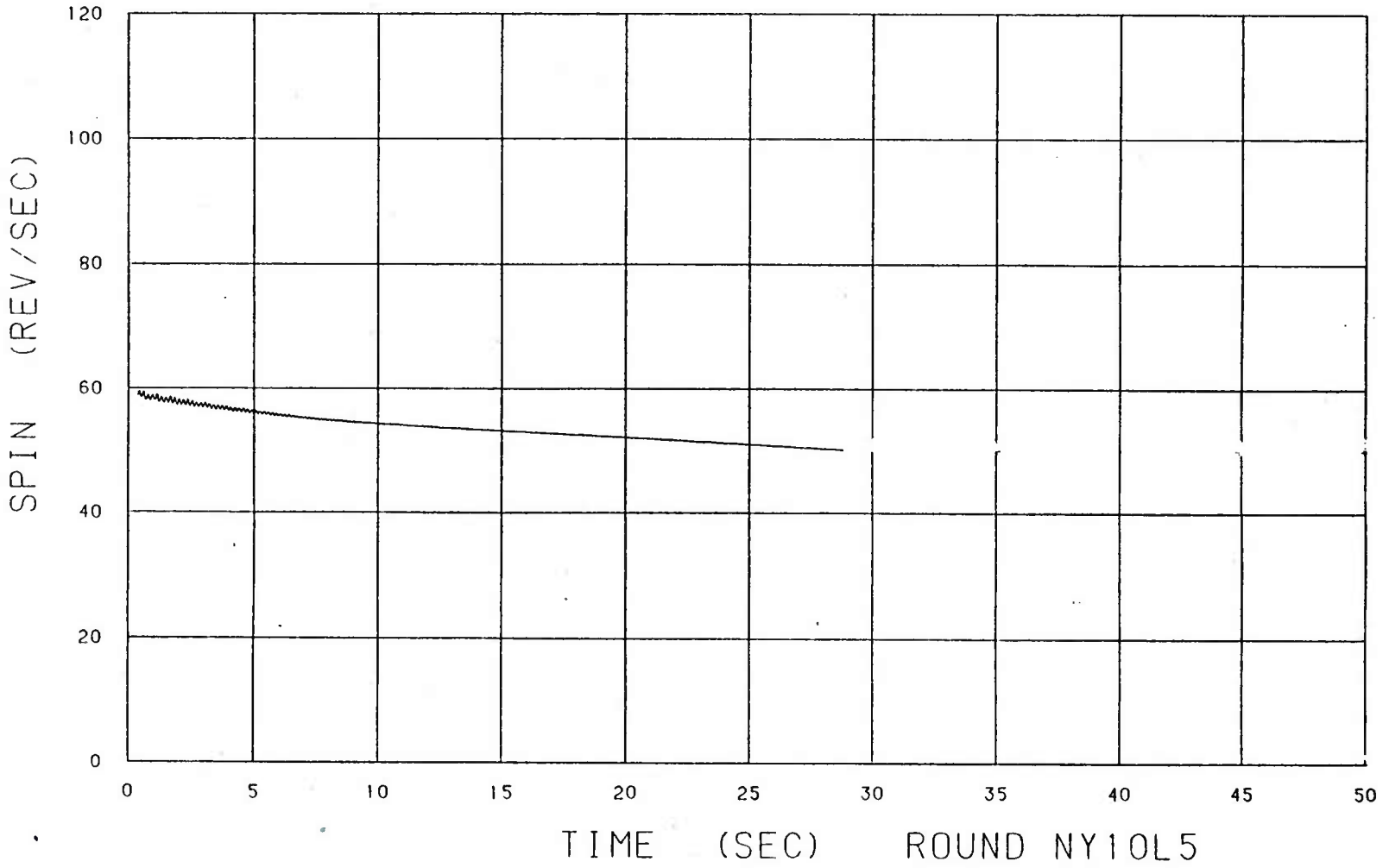

Figure 31. Spin versus Time for Round NY10L5.

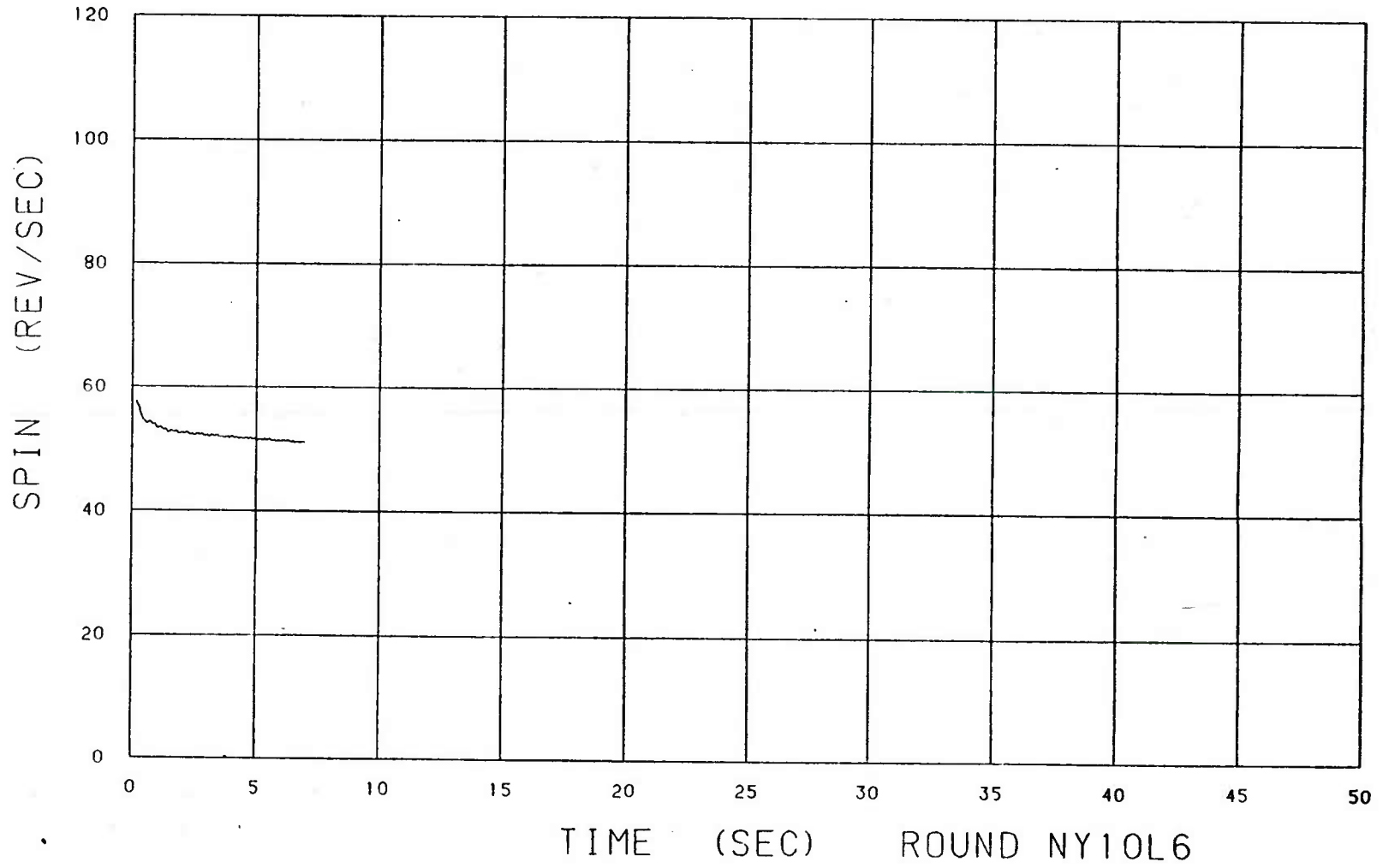

Figure 32. Spin versus Time for Round NY10L6.

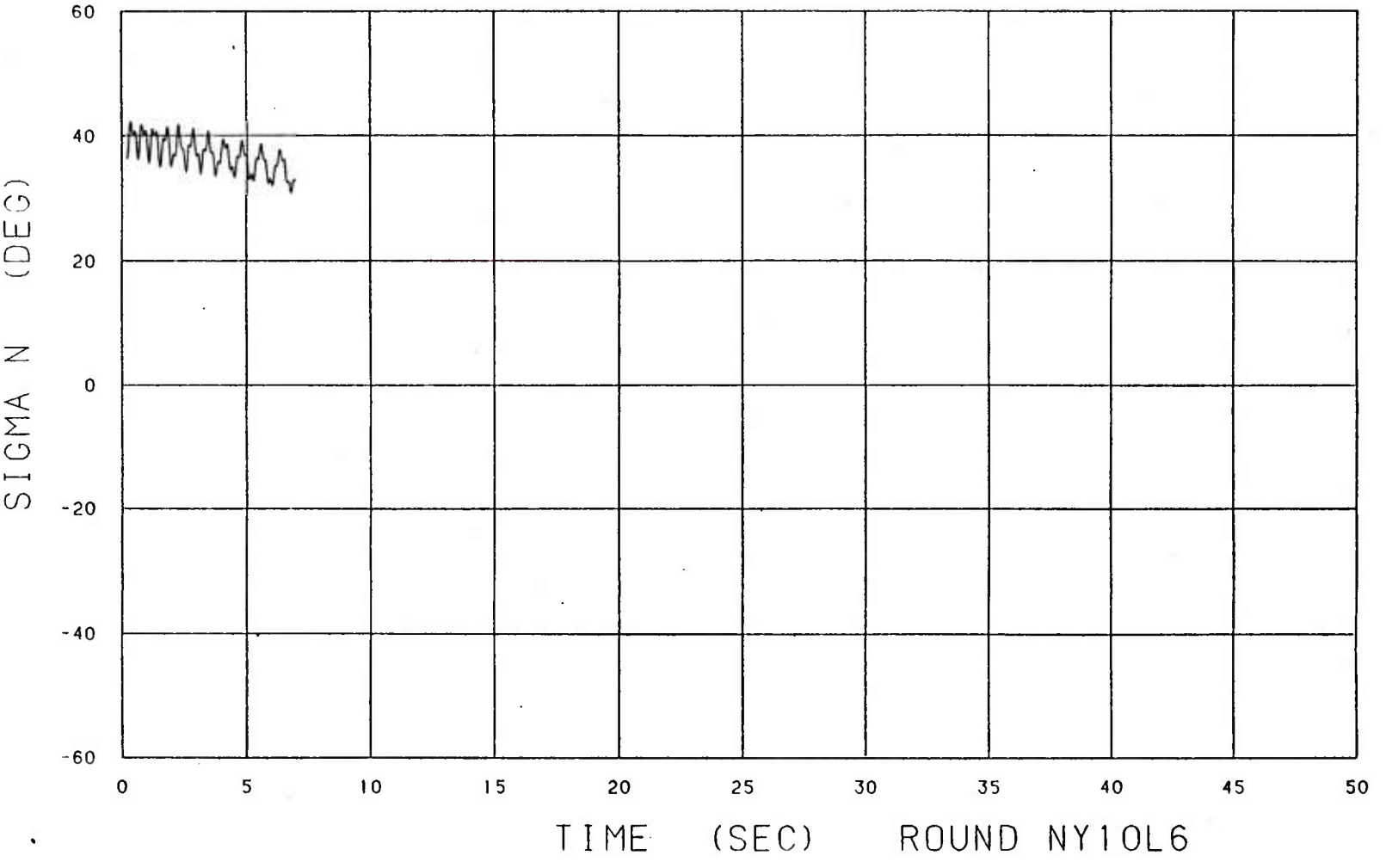

Figure 33. Sigma N versus Time for Round NY10L6.

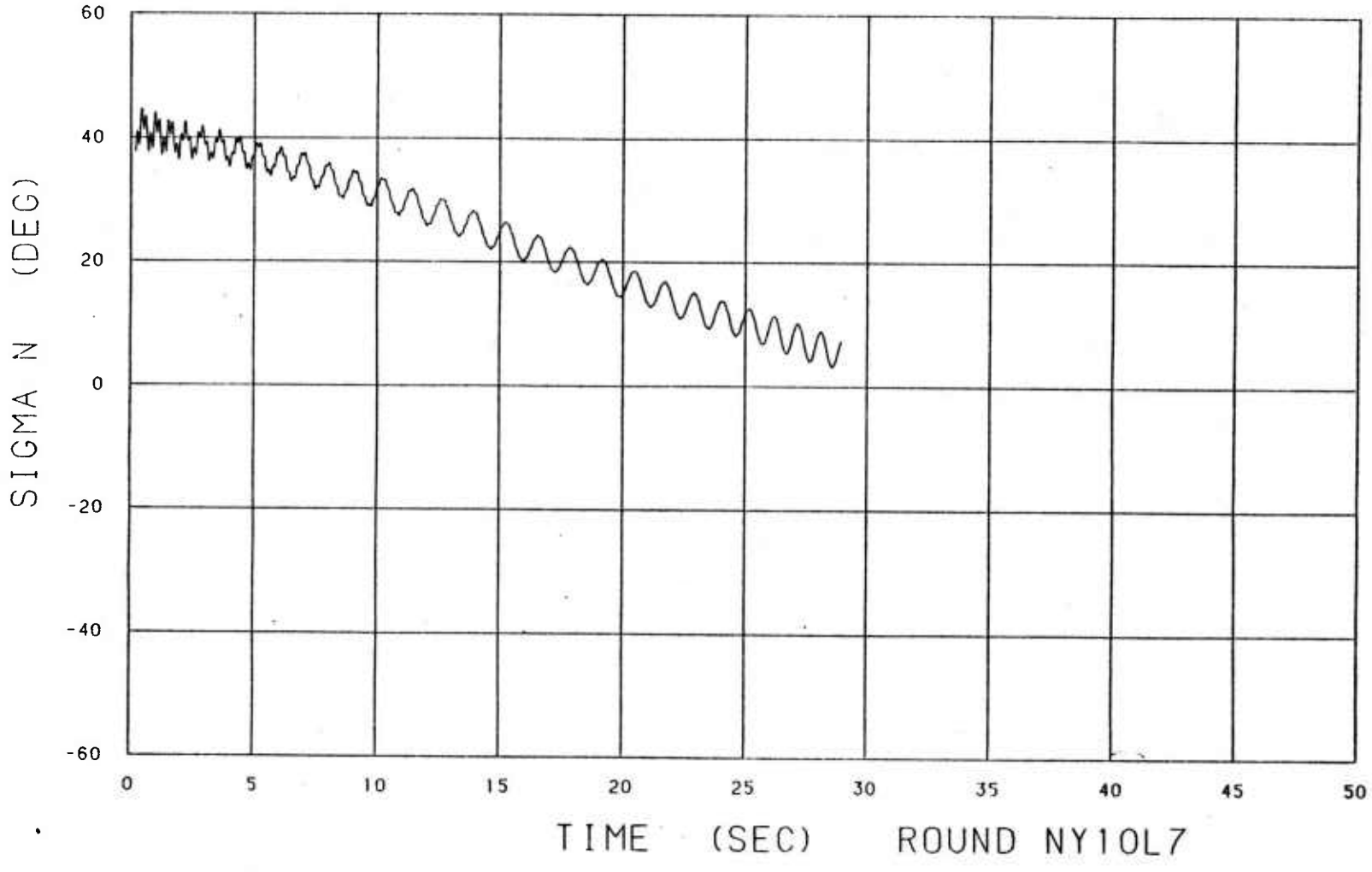

Figure 34. Sigma N versus Time for Round NY10L7.

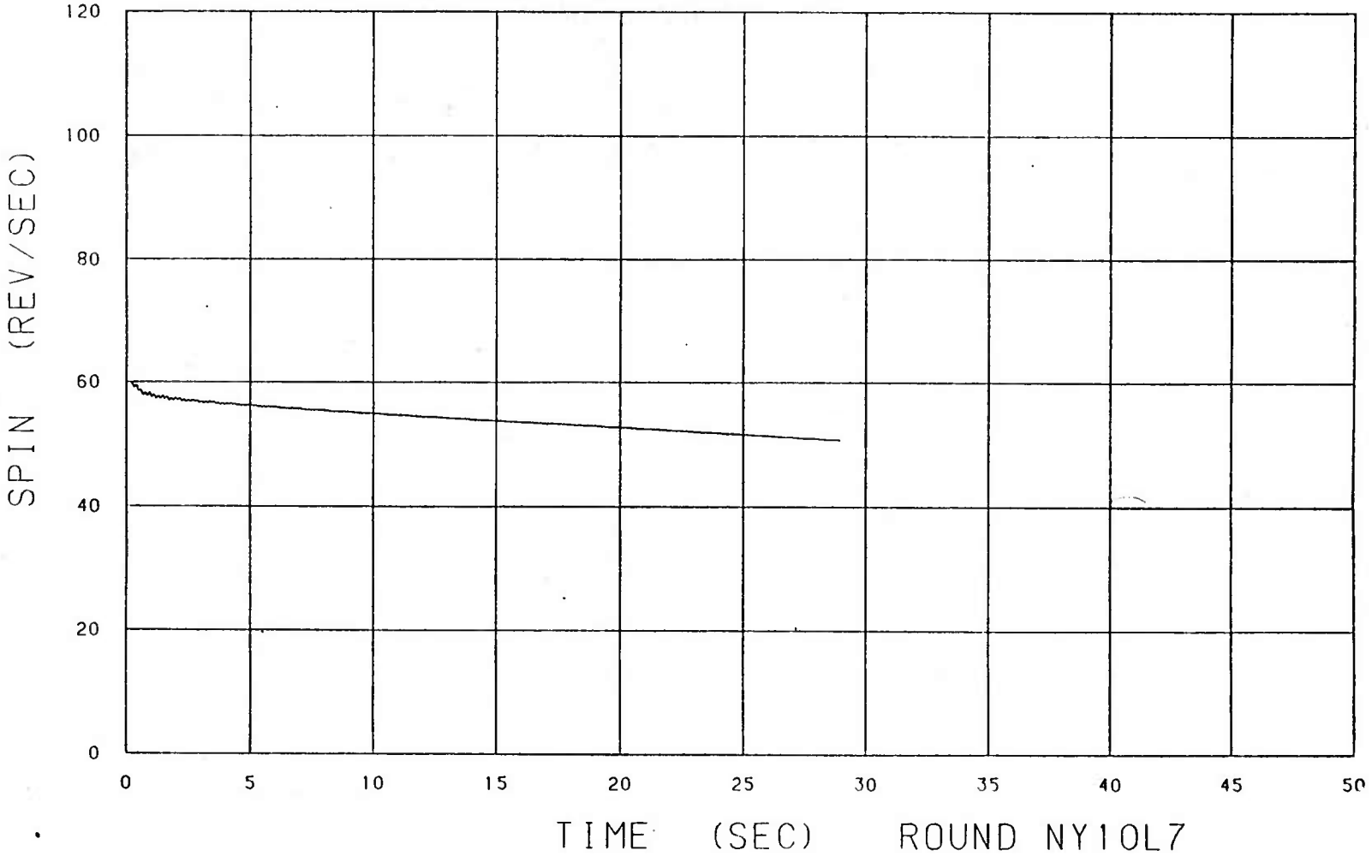

Figure 35. Spin versus Time for Round NY10L7.

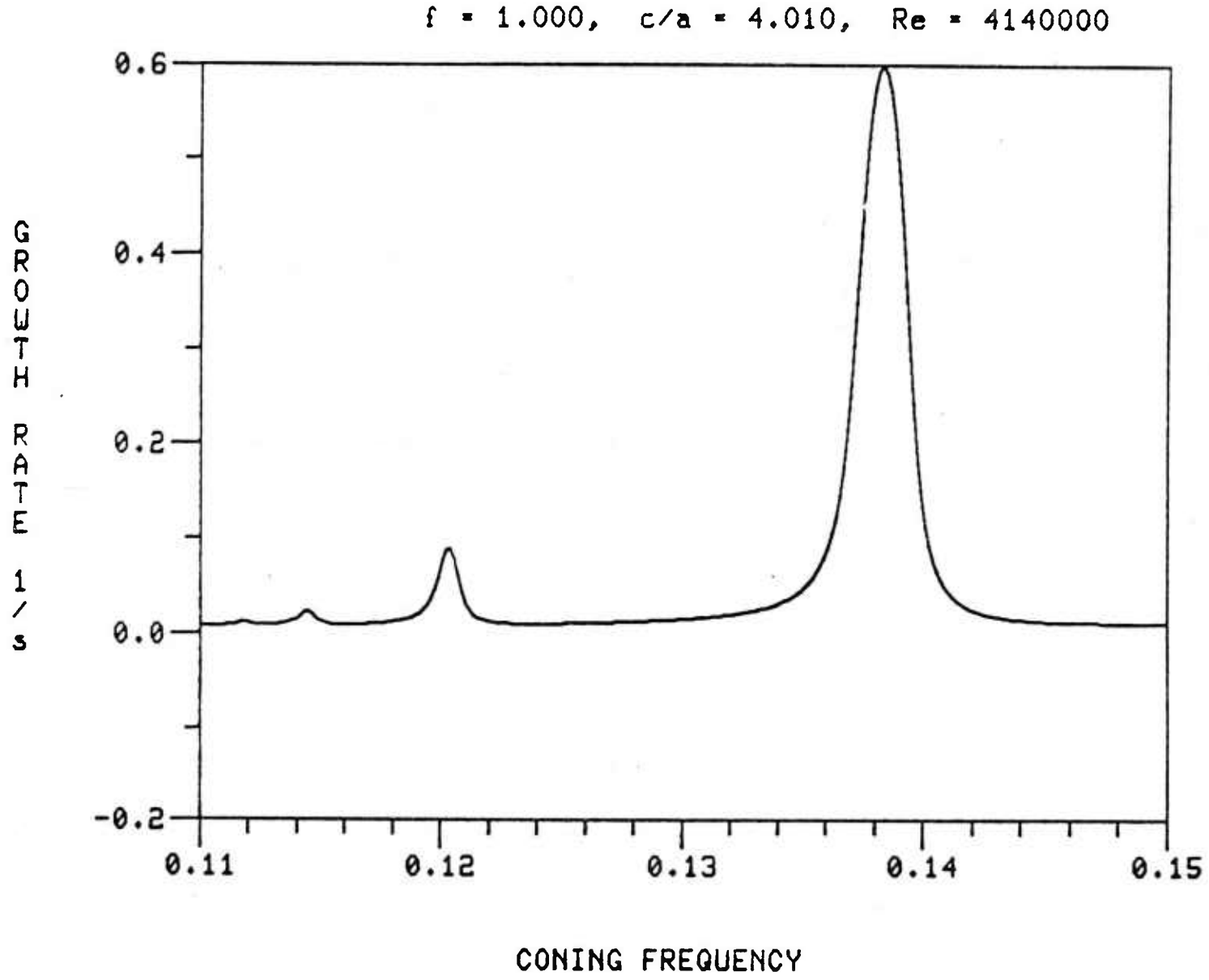

Figure 36. Liquid-Induced Growth Rate Versus Coning Frequency Neglecting Aerodynamic Effects.

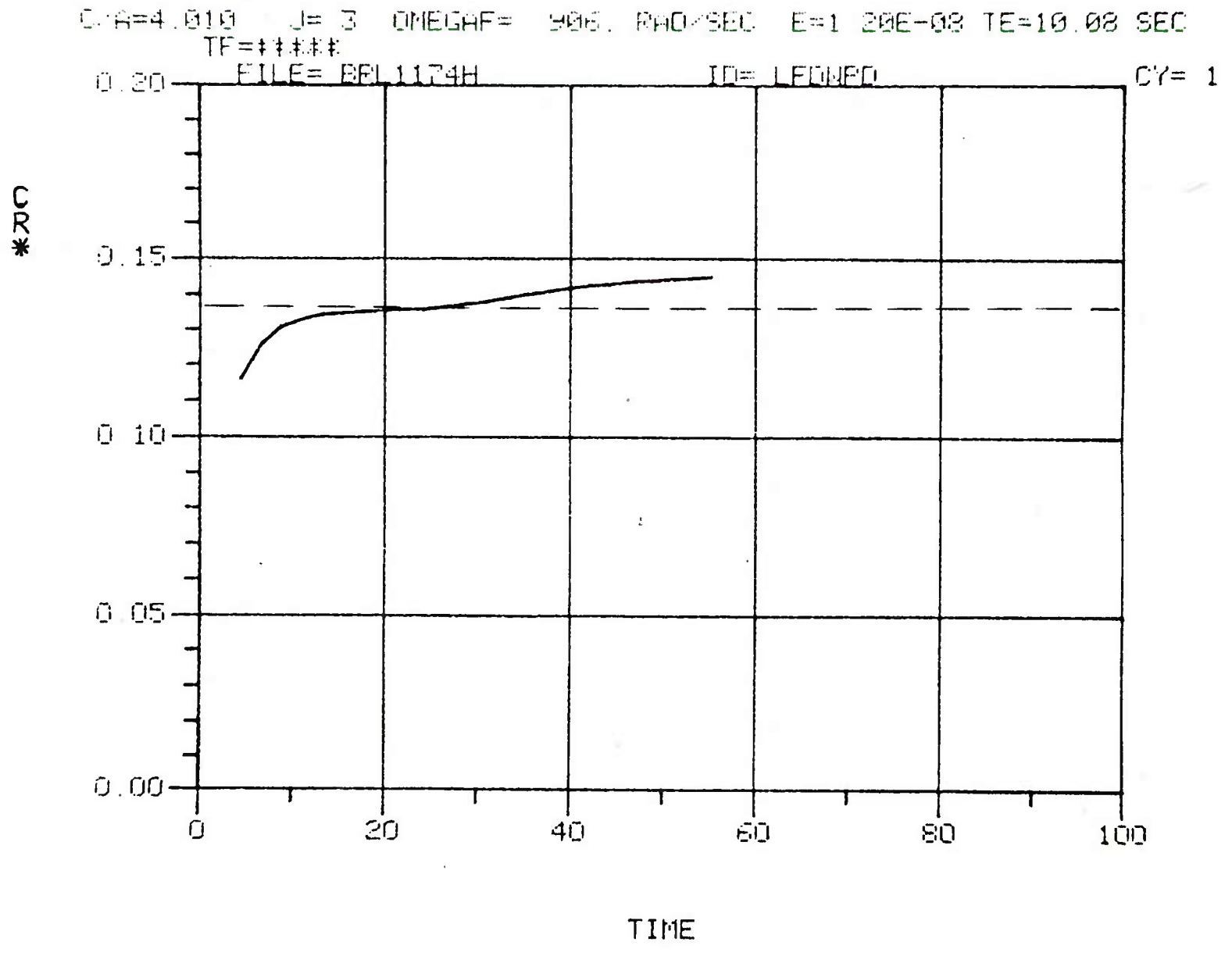

Figure 37. Spin-Up Eigenfrequency History for the (2,3) Mode.

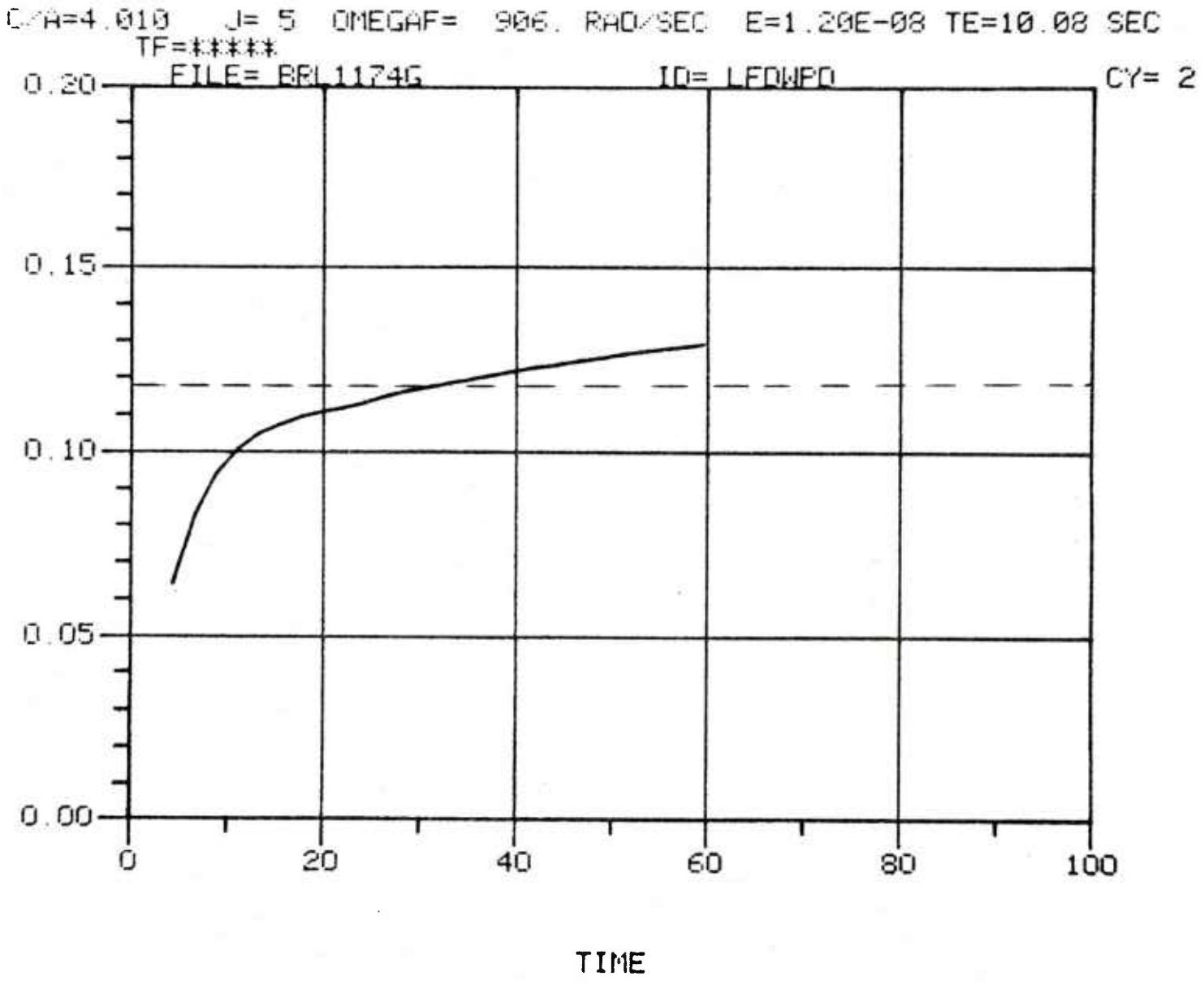

Figure 38. Spin-Up Eigenfrequency History for the (3,5) Mode.

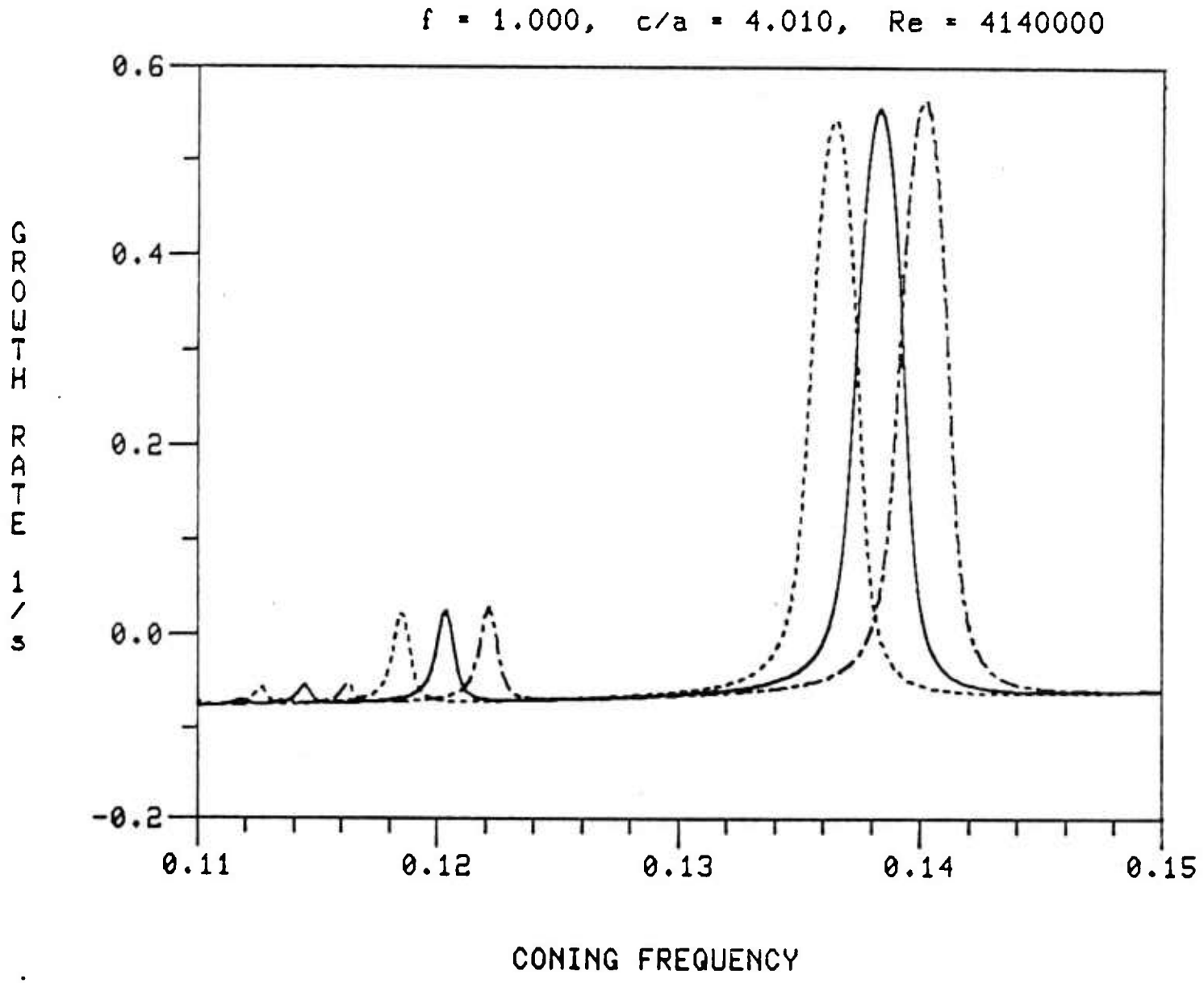

Figure 39. Liquid-Induced Growth Rate Versus Coning Frequency With Aerodynamic Effects.

DISTRIBUTION LIST

No. of Copies	Organization
12	Administrator Defense Technical Info Center ATTN: DTIC-DDA Cameron Station Alexandria, VA 22314
1	Commander US Army Materiel Development and Readiness Command ATTN: DRCDMD-ST 5001 Eisenhower Avenue Alexandria, VA 22333
1	Commander US Army Armament Research and Development Command ATTN: DRDAR-TDC (Dr. D. Gyorog) Dover, NJ 07801
2	Commander US Army Armament Research and Development Command ATTN: DRDAR-TSS (2 cys) Dover, NJ 07801
1	Commander US Army Armament Research and Development Command ATTN: DRDAR-LC, Dr. J. Frasier Dover, NJ 07801
2	Commander US Army Armament Research and Development Command ATTN: DRDAR-LCA-F Mr. D. Mertz Mr. A. Loeb Dover, NJ 07801
1	Commander US Army Armament Materiel Readiness Command ATTN: DRSAR-LEP-L, Tech Lib Rock Island, IL 61299
1	Director US Army Armament Research and Development Command Benet Weapons Laboratory ATTN: DRDAR-LCB-TL Watervliet, NY 12189
1	Commander US Army Aviation Research and Development Command ATTN: DRDAV-E 4300 Goodfellow Blvd St. Louis, MO 63120
1	Director US Army Air Mobility Research and Development Laboratory Ames Research Center Moffett Field, CA 94035
1	Commander US Army Communications Research and Development Command ATTN: DRDCO-PPA-SA Fort Monmouth, NJ 07703
1	Commander US Army Electronics Research and Development Command Technical Support Activity ATTN: DELSD-L Fort Monmouth, NJ 07703
1	Commander US Army Missile Command ATTN: DRSMI-R Redstone Arsenal, AL 35898
1	Commander US Army Missile Command ATTN: DRSMI-YDL Redstone Arsenal, AL 35898
1	Commander US Army Tank Automotive Research and Development Command ATTN: DRDTA-UL Warren, MI 48090

DISTRIBUTION LIST

No. of Copies	Organization
3	Project Manager Cannon Artillery Weapons Systems ATTN: DRCPM-CAWS US Army Armament Research and Development Command Dover, NJ 07801
1	Director US Army TRADOC Systems Analysis Activity ATTN: ATAA-SL, Tech Lib White Sands Missile Range NM 88002
2	Sandia Laboratories ATTN: W.L. Oberkampf H. Vaughn Albuquerque, NM 87115
1	Aerospace Corporation Aero-Engineering Subdivision ATTN: Walter F. Reddall El Segundo, CA 90245
2	Calspan Corporation ATTN: G. Homicz W. Rae P.O. Box 400 Buffalo, NY 14225

No. of Copies	Organization
	Aberdeen Proving Ground
	Director, USAMSAA ATTN: DRXSY-D DRXSY-MP, H. Cohen
	Commander, USATECOM ATTN: DRSTE-TO-F
	PM SMOKE, Bldg. 324 ATTN: DRCPM-SMK
	Director, USACSL, EA Bldg. E3330 ATTN: J. McKivrigan W. Dee
	Director, USACSL, EA Bldg. E3516 ATTN: DRDAR-CLB-PA (1 cy) M. Miller (1 cy)

USER EVALUATION OF REPORT

Please take a few minutes to answer the questions below; tear out this sheet, fold as indicated, staple or tape closed, and place in the mail. Your comments will provide us with information for improving future reports.

1. BRL Report Number _____

2. Does this report satisfy a need? (Comment on purpose, related project, or other area of interest for which report will be used.)

_____

_____

_____

3. How, specifically, is the report being used? (Information source, design data or procedure, management procedure, source of ideas, etc.) _____

_____

_____

4. Has the information in this report led to any quantitative savings as far as man-hours/contract dollars saved, operating costs avoided, efficiencies achieved, etc.? If so, please elaborate.

_____

_____

5. General Comments (Indicate what you think should be changed to make this report and future reports of this type more responsive to your needs, more usable, improve readability, etc.) _____

_____

_____

_____

6. If you would like to be contacted by the personnel who prepared this report to raise specific questions or discuss the topic, please fill in the following information.

Name: _____

Telephone Number: _____

Organization Address: _____

_____

_____